HHS Public Access

Author manuscript

J Med Chem. Author manuscript; available in PMC 2020 May 09.

Published in final edited form as:

J Med Chem. 2019 May 09; 62(9): 4755–4771. doi:10.1021/acs.jmedchem.9b00508.

D_2 Dopamine Receptor G Protein-Biased Partial Agonists Based on Cariprazine

Yudao Shen[†,#], **John D. McCorvy**[‡,§,#], **Michael L. Martini**[†], **Ramona M. Rodriguiz**[‖], **Vladimir M. Pogorelov**[‖], **Karen M. Ward**[⊥], **William C. Wetsel**[‖], **Jing Liu**[*,†], **Bryan L. Roth**[*,‡], and **Jian Jin**[*,†]

[†]Mount Sinai Center for Therapeutics Discovery, Departments of Pharmacological Sciences and Oncological Sciences, Tisch Cancer Institute, Icahn School of Medicine at Mount Sinai, New York, New York 10029, United States

[‡]Department of Pharmacology and National Institute of Mental Health Psychoactive Drug Screening Program, School of Medicine, University of North Carolina at Chapel Hill, Chapel Hill, North Carolina 27599, United States

[§]Department of Cell Biology, Neurobiology and Anatomy, Medical College of Wisconsin, Milwaukee, Wisconsin 53226, United States

[‖]Departments of Psychiatry and Behavioral Sciences, Cell Biology, and Neurobiology, Duke University Medical Center, Durham, North Carolina 27710, United States

[⊥]Worldwide Research and Development, Internal Medicine Research Unit, Pfizer, Cambridge, Massachusetts 02139, United States

Abstract

Functionally selective G protein-coupled receptor ligands are valuable tools for deciphering the roles of downstream signaling pathways that potentially contribute to therapeutic effects versus side effects. Recently, we discovered both $G_{i/o}$-biased and β-arrestin2-biased D_2 receptor agonists based on the Food and Drug Administration (FDA)-approved drug aripiprazole. In this work, based on another FDA-approved drug, cariprazine, we conducted a structure–functional selectivity relationship study and discovered compound **38** (MS1768) as a potent partial agonist that selectively activates the $G_{i/o}$ pathway over β-arrestin2. Unlike the dual D_2R/D_3R partial agonist cariprazine, compound **38** showed selective agonist activity for D_2R over D_3R. In fact, compound **38** exhibited potent antagonism of dopamine-stimulated β-arrestin2 recruitment. In our docking studies, compound **38** directly interacts with $S193^{5.42}$ on TM5 but has no interactions with extracellular loop 2, which appears to be in contrast to the binding poses of D_2R β-arrestin2-biased ligands. In in vivo studies, compound **38** showed high D_2R receptor occupancy in mice and effectively inhibited phencyclidine-induced hyperlocomotion.

[*]**Corresponding Authors** jian.jin@mssm.edu (J.J.). bryan_roth@med.unc.edu (B.L.R.). jing.liu@mssm.edu (J.L.).

[#]Y.S. and J.D.M. contributed equally to this work.

Supporting Information

The Supporting Information is available free of charge on the ACS Publications website at DOI: 10.1021/acs.jmedchem.9b00508.

^1H and ^{13}C NMR spectra of compound **38** (PDF) Molecular formula strings and some data (CSV)

The authors declare the following competing financial interest(s): K.M.W. was an employee of Pfizer.

Graphical Abstract

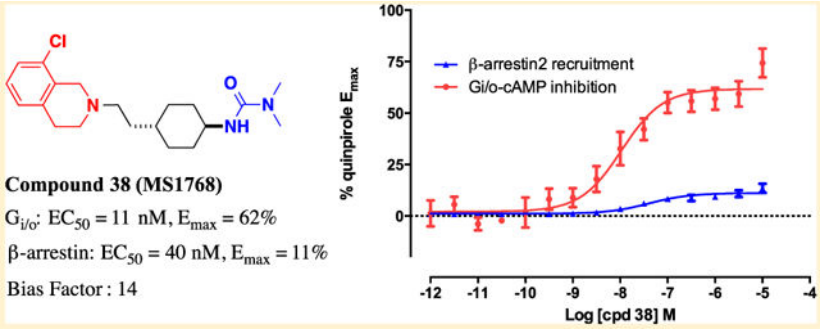

INTRODUCTION

G protein-coupled receptors (GPCRs) are seven-transmembrane domain receptors[1] that have been implicated in the pathophysiology of numerous human diseases including schizophrenia,[2] Parkinson's disease,[3] attention-deficit disorders,[4] and obesity.[5] More than 30% of current Food and Drug Administration (FDA) approved drugs target GPCRs. [1,6,7] Historically, GPCR drug discovery has postulated that ligand engagement with a receptor could only lead to a single unique outcome.[1] Under this simplified paradigm, partial and full agonists were classified as ligands that stimulated the recognized downstream signaling pathway, whereas antagonists were ligands that simply blocked the actions of agonists.[8] Current research, however, suggests that GPCR ligands can induce conformational changes that result in selective activation of distinct downstream signaling pathways.[1, 7] This concept has been widely accepted by the academic and pharmaceutical communities and is termed biased signaling or functional selectivity.[9–14]

Functional selectivity in GPCR ligands has important potential clinical implications as it has been suggested that different signaling pathways contribute to various drug pharmacological profiles including both therapeutic actions and adverse effects.[15–17] For example, carvedilol and metoprolol tartrate are both inverse agonists of cyclic adenosine monophosphate (cAMP) production at β_2AR, but carvedilol has also been shown to possess phospho-ERK1/2 activity, likely leading to the reduction in mortality observed in a clinical trial on patients with chronic heart failure.[18,19] Another example includes PZM21, a potent Gi-biased agonist of the μ-opioud-receptor (μOR) that was shown to efficiently reduce pain without causing lethal side effects, such as fatal respiratory depression and morphine-like reinforcing activity. In contrast, both of these side effects are observed alongside therapeutic analgesia when the unbiased μOR agonist morphine is administered.[20] These findings have fueled great interest in the discovery of new functionally selective ligands for various GPCRs.[13,21–36]

Dopaminergic receptors are a subfamily of aminergic GPCRs that are highly expressed in the brain. Dopaminergic receptors are generally classified into subtypes as D_1-like (D_1 and D_5) and D_2-like (D_2, D_3, and D_4). D_2R is the most highly studied dopaminergic receptor due to its implication in neuropsychiatric diseases.[37,38] Previously, we discovered both β-arrestin2-biased and G protein-biased D_2R agonists through investigation of the structure–

functional selectivity relationship (SFSR) of the FDA-approved drug aripirazole.[35,39–41] Other groups have also reported multiple functionally selective D_2 receptor agonists.[27–30,42–45] Among them, cariprazine and its 1,2,3,4-tetrahydroisoquinoline (THIQ) isosteres were reported to selectively activate the D_2R $G_{i/o}$-mediated cAMP inhibition pathway over the phospho-ERK1/2 pathway.[27] However, for these cariprazine analogues, there are no reports on ligand bias with regard to β-arrestin recruitment.

Cariprazine is an FDA-approved drug for the treatment of schizophrenia and bipolar mania in adults and is currently also under clinical investigation for the treatment of bipolar depression and major depressive disorder.[46] Cariprazine, however, is also known to carry several side effects including extrapyramidal symptoms, indigestion, nausea, headache, and weight gain.[47] A functionally selective cariprazine-biased D_2R agonist has the potential to serve as a tool for dissecting the therapeutic and adverse effects of different downstream pathways, which may ultimately lead to improved therapeutics. In the present study, we conducted an SFSR study starting from the cariprazine scaffold and report the discovery of compound **38**, a THIQ isostere of cariprazine, as a G protein-biased D_2R partial agonist. Here, we present the design, synthesis, and biological characterization of compound **38** and its analogues.

RESULTS AND DISCUSSION

Discovery of Compound 16 as a G Protein-Biased Agonist.

We conducted an SFSR study on three regions of the cariprazine scaffold: (1) the left-hand side (LHS) 2,3-dichlorophenylpiperazinyl moiety, (2) the middle linker cyclohexylene ring moiety, and (3) the right-hand side (RHS) urea moiety, including a few known compounds in ref 26. The syntheses of **9** (cariprazine) and the designed analogues, **10**–**12**, **15** and **16** are outlined in Schemes 1 and 2. The Boc-protected ethyl 2-(*trans*-4-aminocyclohexyl)acetate **1** was prepared by esterification of commercially available 2-(*trans*-4-aminocyclohexyl)acetic acid, followed by protection of the amino group with di-*tert*-butyl dicarbonate. Lithium borohydride-mediated reduction of the methyl ester provided the alcohol **2**. After activation of the hydroxyl group, the resulting reactive methanesulfonate ester intermediate was converted into the cyano compound **3**. Diisobutylaluminium hydride (DIBAL-H)-mediated reduction of the cyano group afforded the *trans*-aldehyde **4**. The *cis*-aldehyde **8** was synthesized from 2-(*cis*-4-aminocyclohexyl)acetic acid using the same procedures described above for the preparation of compound **4**. Compound **10** was obtained via reductive amination of **4** and 1-(2,3-dichlorophenyl)piperazine in the presence of sodium triacetoxyborohydride. Boc-group deprotection under acidic conditions afforded compound **11**, which was subsequently converted to **9** by dimethylurea formation with dimethylcarbamoyl chloride. Compound **12** was prepared from the *cis*-aldehyde **8** using the same procedures as compound **9**. Compound **15** was synthesized using a 5-carbon linker moiety. Boc protection of commercially available 5-aminopentanol gave **13**. Activation of the free hydroxyl group followed by substitution with 2,3-dichlorophenylpiperazine yielded **14**. Boc deprotection followed by dimethylurea formation afforded compound **15** (Scheme 1). Compound **16** was prepared from the *cis*-aldehyde **4** and 1,2,3,4-tetrahydroisoquinoline using the same procedures as compound **9** (Scheme 2).

All of these synthesized compounds were then evaluated for their effects on D_2R $G_{i/o}$-mediated cAMP inhibition and β-arrestin2 recruitment. The D_2R $G_{i/o}$-mediated cAMP inhibition assay measures inhibition of isoproterenol-stimulated cAMP production via the $G_{i/o}$-coupled signaling pathway, whereas the D_2R-mediated β-arrestin2 translocation Tango assay measured the recruitment of β-arrestin2 to D_2R.[41,48] Quinpirole, a full D_2R agonist, was used as a balanced positive control in both assays ($G_{i/o}$: EC_{50} = 1.8 nM, pEC_{50} = 8.74 ± 0.08; β-arrestin2: EC_{50} = 2.7 nM, pEC_{50} = 8.57 ± 0.10). The potency (EC_{50}) and efficacy (E_{max}) in both pathways for each compound in this series are displayed in Table 1.

Although compound **9** was reported to be functionally selective for the cAMP ($G_{i/o}$-protein) pathway over the ERK1/2 phosphorylation pathway,[27] this compound did not show significant bias for the $G_{i/o}$ pathway (EC_{50} = 0.4 nM; E_{max} = 70%) over the β-arrestin2 pathway (EC_{50} = 0.6 nM; E_{max} = 66%). Modification of the dimethylurea group to a *tert*-butyl carbamate (**10**) drastically reduced the potencies for both the $G_{i/o}$ (35-fold) and β-arrestin2 (15-fold) pathways, while slightly increasing the efficacies to approximately 75% of the maximal responsiveness in both pathways. Truncation of the dimethylurea group to the primary amino group (**11**) did not obviously change either potency or efficacy for the $G_{i/o}$ pathway. Compared to **9**, compound **11** displayed decreased potency (3-fold) and retained almost equal efficacy in the β-arrestin2 recruitment assay, suggesting that a positively charged amino group in this region is detrimental to potency in β-arrestin2 recruitment. Switching the *trans*-1,4-cyclohexylene of **9** to a *cis*-1,4-cyclohexylene moiety (**12**) resulted in a significant decrease in the potency and efficacy in both the $G_{i/o}$ and β-arrestin2 pathways ($G_{i/o}$: EC_{50} = 3 nM; E_{max} = 48%; β-arrestin2: EC_{50} = 12 nM; E_{max} = 37%). Replacement of the *trans*-1,4-cyclohexylene group-containing linker to a more flexible 5-carbon chain led to a significant decrease in potency (17-fold) and efficacy (E_{max} = 24%) for β-arrestin2 recruitment and also an obvious decrease in potency (18-fold) and efficacy (E_{max} = 29%) for the $G_{i/o}$ pathway. Replacement of the 2,3-dichlorophenylpiperazine to its isostere 1,2,3,4-tetrahydroisoquinoline (THIQ) has been explored in D_2R and D_3R studies.[27,49] The THIQ compound **16** displayed significantly reduced potency and efficacy in both pathways ($G_{i/o}$: EC_{50} = 12 nM; E_{max} = 60%; β-arrestin2: EC_{50} = 69 nM; E_{max} = 22%). However, **16** also displayed bias toward $G_{i/o}$ signaling over β-arrestin2 recruitment with a bias factor of 11 relative to quinpirole.

Given the promising functional selectivity of **16**, we opted to focus our SFSR campaign on the THIQ series by exploring three regions of this scaffold: the LHS 1,2,3,4-tetrahydroisoquinoline moiety, the middle linker cyclohexylene ring moiety, and the RHS urea moiety.

SFSR of the RHS of the THIQ Scaffold.

We explored a series of compounds (**17**–**25**) with different sized urea, carbamate, and amide moieties at the RHS. These compounds were synthesized according to the procedures for the preparation of **16**, as outlined in Scheme 2. The results from both cAMP and β-arrestin2 assays are summarized in Table 2.

Increasing the bulkiness of the dimethylurea moiety (**16**) to diethylurea (**17**) or diisopropyl urea (**18**) significantly reduced the potencies by 3–5-fold, while maintaining the maximal responsiveness for both the $G_{i/o}$ and β-arrestin2 recruitment pathways. Compared to **16**, a pyrrolidine carboxamide group (**19**) retained similar potency and increased the efficacy ($G_{i/o}$: EC_{50} = 14 nM; E_{max} = 66%; β-arrestin2: EC_{50} = 88 nM; E_{max} = 42%) in both pathways. This modification, however, did not improve the bias profile toward $G_{i/o}$ protein activity. For the carbamate analogues, the *tert*-butyl group (**20**) showed better $G_{i/o}$ pathway activation (EC_{50} = 33 nM; E_{max} = 59%) than isopropyl (**21**) (EC_{50} = 74 nM; E_{max} = 49%) and ethyl groups (EC_{50} = 144 nM; E_{max} = 53%). Similarly, the *tert*-butyl group (**20**) also demonstrated better activity in the β-arrestin2 recruitment assay (EC_{50} = 195 nM; E_{max} = 52%) than isopropyl (**21**) (EC_{50} = 238 nM; E_{max} = 26%) and ethyl (**22**) groups (EC_{50} = 636 nM; E_{max} = 22%). For the amide RHS, benzamide (**23**) was more potent in inducing both $G_{i/o}$-mediated cAMP inhibition (EC_{50} = 8 nM; E_{max} = 62%) and β-arrestin2 recruitment (EC_{50} = 65 nM; E_{max} = 50%) than propionamide (**24**) and acetamide (**25**). Albeit rather weak agonists for the $G_{i/o}$ pathway (for **24**: EC_{50} = 132 nM; E_{max} = 33%; for **25**: EC_{50} = 54 nM; E_{max} = 22%), both propionamide (**24**) and acetamide (**25**) showed diminished efficacy in β-arrestin2 recruitment (EC_{50} not calculated; E_{max} < 10%). Consequently, these smaller amide moieties (**24** and **25**) confer apparent functional selectivity toward the $G_{i/o}$ pathway.

Overall, this SFSR study with the urea, carbamate, and amide moieties of the THIQ scaffold did not provide a significantly superior functionally selective D_2R agonist compared to compound **16**. Modifications that lead to improved activities in the $G_{i/o}$ pathway were always accompanied with improved β-arrestin2 recruitment. To improve the functional selectivity and efficacy of this series in the $G_{i/o}$ pathway, we retained the dimethylurea moiety of compound **16** for the following studies on the middle linkers and LHS moieties.

SFSR of the Middle Linker of the THIQ Scaffold.

To determine effects of the middle linker on D_2R functional selectivity, we explored compounds **26**, **28**, **30**, and **32**. The synthetic routes are summarized in Scheme 3. Their biological results are outlined in Table 3.

Compound **26** was synthesized according to the same procedures for the preparation of **16** from the *cis*- aldehyde **8**. The preparation of compound **28** started from compound **2**. The activation of the hydroxyl group of **2** with methanesulfonyl chloride, followed by substitution with 1,2,3,4-tetrahydroisoquinoline, provided the Boc-protected intermediate **27**. Boc deprotection and subsequent urea formation yielded **28**. Compound **30** was synthesized following the protocols for the preparation of **28** from the alcohol intermediate **29**, which was prepared by selective Boc protection of the commercially available 2-(4-aminophenyl)-ethan-1-ol. Similarly, compound **32** was synthesized using the same route as the preparation of **28** from the alcohol **13** (Scheme 3).

Replacement of the *trans*-1,4-cyclohexylene ring of **16** with a *cis*-1,4-cyclohexylene group (**26**) significantly decreased potency (22-fold), while maintaining efficacy (E_{max} = 58%) for the $G_{i/o}$ pathway. Interestingly, compound **26** showed very low activity for β-arrestin2 recruitment (EC_{50} > 1000 nM), resulting in our inability to calculate a bias factor for this

compound. However, **26** still showed low potency for the $G_{i/o}$ pathway (EC_{50} = 259 nM), indicating weak G protein-bias. Incorporation of a short linker (**28**), a rigid aromatic linker (**30**), or a flexible 5-C chain linker (**32**) resulted in compounds that were all inactive in both the cAMP inhibition and β-arrestin2 recruitment assays. Taken together, these findings suggest that the central linker plays an important role in the functional potency and efficacy of this scaffold in both the $G_{i/o}$ and β-arrestin2 signaling pathways.

SFSR of the LHS of the THIQ Scaffold.

We next explored compounds **33**–**43** to study the effects of phenyl substituents on D_2R functional selectivity. Compounds **33**–**43** were prepared using the same synthetic routes for **16**, starting from the appropriately substituted 1,2,3,4-tetrahydroisoquinoline precursor (Scheme 4). The biological assay data are summarized in Table 4.

Given that cariprazine featured a dichloro substitution pattern on its LHS, we designed and synthesized compound **33** bearing a 5,6-dicholoro-substituted THIQ. Similar to cariprazine, compound **33** was not functionally selective in the two signaling pathways. Notably, however, this compound exhibited higher efficacy than cariprazine for both the $G_{i/o}$ (E_{max} = 116%) and β-arrestin2 (E_{max} = 90%) pathways. In fact, its $G_{i/o}$ signaling efficacy was even higher than that of the control compound quinpirole (E_{max} = 100%), indicating superagonism. A 6,7-dioxole on the THIQ (**34**) did not show significant $G_{i/o}$ pathway selectivity. Because of the enhanced maximal responsiveness of both signaling pathways to the 5,6-dichloro substituent (**33**), we explored the effects of monochloro substituents at the 5-, 6-, 7-, and 8-positions on the THIQ. Similar to **33**, the 5-chloro compound **35** was a balanced near-full agonist for both the $G_{i/o}$ signaling pathway (E_{max} = 95%) and β-arrestin2 recruitment (E_{max} = 92%). A monochloro substituent at the 7-position (**37**) also resulted in a balanced effect in both pathways, however, a 6- or 8-chloro substituent on the THIQ moiety led to biased partial agonists for activating $G_{i/o}$ signaling. Although the functional selectivity of **36** (6-chloro) was moderate, compound **38** (8-chloro) displayed enhanced bias toward activating the $G_{i/o}$ signaling pathway (EC_{50} = 11 nM; E_{max} = 62%) over β-arrestin2 recruitment (EC_{50} = 40 nM; E_{max} = 11%) with a bias factor of 14. We next explored the methyl (**39**), bromo (**40**), fluoro (**41**), trifluoromethyl (**42**), and methoxy (**43**) substituents at the 8-position. Albeit with lower functional potencies (27–86 nM) for the $G_{i/o}$ signaling pathway than **38**, all of these compounds appeared to be partial agonists for stimulating $G_{i/o}$ signaling. Taken together, our results suggest that the substituents of the LHS 1,2,3,4-tetrahydroisoquinoline moiety play a critical role in modulating functional selectivity of D_2R. The 8-chloro substituent on the THIQ moiety provided a potent and $G_{i/o}$-biased compound, **38**.

Evaluation of $G_{i/o}$ Protein-Biased D_2R Agonist 38 in Orthogonal Assays.

To further confirm the observed signaling bias, which has been shown to depend on cell background and readout.[14,50] we tested **38** in a bioluminescence resonance energy transfer (BRET)-based assay[51] using quinpirole as the control. As demonstrated in Figure 1A, in HEK 293T cells co-expressing D_2R C-terminal tagged renilla luciferase (Rluc), a Venus-tagged β-arrestin2, and G protein-coupled receptor kinase 2 (GRK2), compound **38** displayed no activity for D_2R-mediated β-arrestin2 recruitment compared to quinpirole

(EC_{50} = 115 nM; E_{max} = 100%). Next, to confirm compound **38** is an agonist in the D_2R G protein pathway, we tested compound **38** in a $G\alpha i1$–$G\gamma 2$ dissociation BRET-based assay[52] using quinpirole as a control. In this assay, compound **38** showed potent partial agonist activity (EC_{50} = 0.40 nM; E_{max} = 47%) compared to quinpirole (EC_{50} = 2.4 nM; E_{max} = 100%) (Figure 1B). Taken together, BRET-based orthologous assay platforms for either G protein activation or β-arrestin2 recruitment confirmed that compound **38** is a G protein-biased D_2R partial agonist.

Evaluation of $G_{i/o}$ Protein-Biased D_2R Agonist 38 in D_2R β-Arrestin Antagonist Mode and in D_3R Functional Assays.

Considering that compound **38** is a $G_{i/o}$ protein-biased partial agonist showing no activity for D_2R β-arrestin2 activity, we examined the antagonist activity of **38** for dopamine (DA)-induced D_2R β-arrestin2 recruitment. Different from dopamine, compound **38** did not show agonist activity toward β-arrestin2 recruitment (Figure 2A). However, similar to clozapine, **38** exhibited potent antagonism in blocking dopamine-stimulated β-arrestin2 recruitment (Figure 2A).

Because cariprazine is a D_2R/D_3R dual partial agonist, we also tested whether the functionally selective D_2R partial agonist, compound **38**, is also a D_3R agonist. As demonstrated in Figure 2B,C, compound **38** acts as a selective agonist at D_2R over D_3R, showing no agonist activity in D_3R $G_{i/o}$-mediated cAMP inhibition assay (Figure 2B) or β-arrestin2 recruitment assay (Figure 2C).

In Silico Studies.

We next sought to explore how these findings from our SFSR campaign fit into the existing paradigms for biased signaling at D_2R. To do this, we docked cariprazine, **16**, and **38** to a model based on the co-crystal structure of D_2R in the complex with risperidone (PDB: 6CM4).[38] Because antagonists, such as risperidone, may stabilize different receptor conformations compared to agonists, we first compared this model to that of a previous D_2R model from the literature that successfully modeled functional selectivity in D_2R agonists.[41] The all-atom binding site root-mean-square deviation (RMSD) between our present model and this previously reported D_2R model was 0.74 Å,[41] indicating a high degree of similarity between the atom arrangements lining the binding pockets of both structures (Figure 3A).

Cariprazine docked to D_2R revealed key binding pocket interactions including a salt bridge interaction between cariprazine's protonated piperazinyl nitrogen and the conserved $D114^{3.32}$ residue (2.52 Å) and a close edge-to-face π interaction between cariprazine's LHS dichlorophenyl entity and $F390^{6.52}$ (2.89 Å, Figure 3B). Notably in our pose, the LHS dichlorophenyl entity is oriented upward and toward TM5, such that the 3-chloro group can form a hydrogen bond with $S193^{5.42}$ (2.52 Å), which is a residue found to be important for D_2R $G_{i/o}$-dependent signaling.[41] Furthermore, the 3-chloro appears to form an n–π interaction with $F189^{5.38}$, and the 2-chloro group is pointed toward $I184^{EL2}$ (4.70 Å), which is a residue previously implicated in D_2R β-arrestin2 recruitment efficacy.[41,45,53] Taken together, cariprazine's binding pose appears to be consistent with its balanced agonist activity (Figure 3B).

By contrast, D_2R G protein-biased compounds **16** (Figure 3C) and **38** (Figure 3D) appear to dock deeper in the orthosteric binding site, lacking clear interactions with $I184^{EL2}$ and engaging TM5 further via strict steric constraints, which has previously been shown to play an important role in receptor activation and G protein signaling.[54] Specifically, the chloro substitution of **38** is able to directly interact with $S193^{5.42}$ on TM5 (2.07 Å). Given previous findings that ligand engagement with TM5 serines is critical for G protein signaling at D_2R,[41] this binding pose suggests that the TM5–LHS chloro interaction may contribute to **38**'s dramatic increase in $G_{i/o}$ bias compared to **16**, which by comparison has a weaker interaction with TM5. These docking poses suggest that the selective engagement with TM5 over EL2 may be important for the D_2R $G_{i/o}$-bias of compounds **16** and **38**, which is consistent with mechanisms previously proposed in the literature.[41]

Receptor Occupancy and Behavioral Studies in Mice.

To evaluate the in vivo D_2R target engagement of compound **38**, we implemented a radioactive competitive assay to assess the displacement of [^{3}H]-raclopride in mouse striatum and cerebellum.[55] Compound **38** dose-dependently bound to the D_2R in mouse striatum and cerebellum, with full receptor occupancy observed at 32 mg/kg intravenous dose (Figure 4). The high D_2R target engagement of **38** encouraged us to examine the in vivo pharmacological effects of this ligand on supressing the NMDA receptor antagonist phencyclidine (PCP) in a PCP-stimulated hyperlocomotion open field test. Compound **38** significantly reduced PCP-induced hyperlocomotion at 1 mg/kg. At an elevated dose of 3.5 mg/kg, **38** almost completely suppressed the induced hyperlocomotion (Figure 5). It remains unclear whether the suppression of hyperlocomotor activity is due to compound **38**'s G protein-biased agonism or antagonism in this model of high dopamine efflux. Taken together, compound **38** was efficacious in vivo and may serve as a potential in vivo tool compound for elucidating the role of G protein-mediated D_2R signaling.

CONCLUSIONS

In summary, we designed and synthesized a series of cariprazine analogues and evaluated them in cAMP accumulation and β-arrestin2 recruitment assays. Our initial SFSR study revealed compound **16**, bearing a THIQ moiety, which exhibited bias for activating $G_{i/o}$ signaling over β-arrestin2 pathway with a bias factor of 11. Further optimization of **16** led to the discovery of compound **38**, which displayed an enhanced functional selectivity for the $G_{i/o}$ signaling pathway β-arrestin2 recruitment with a bias factor of 14. Orthologous BRET assays were used to confirm that **38** was a G protein-biased partial agonist. Unlike cariprazine, which was a dual partial agonist of D_2R/D_3R, compound **38** showed no agonist activity at D_3R but demonstrated partial $G_{i/o}$ protein agonist activity at D_2R. Compound **38** also exhibited potent D_2R antagonism of dopamine-stimulated β-arrestin2 recruitment. Docking studies suggested that both a TM5–LHS chloro interaction and the resulting scaffold separation from EL2 could contribute to **38**'s high functional selectivity in the $G_{i/o}$ pathway. Finally, compound **38** was assessed in an in vivo receptor occupancy assay and a psychotomimetic-induced hyperlocomotion assay in rodents. Compound **38** showed high in vivo D_2R target engagement as well as dose-dependent inhibition of PCP-induced hyperlocomotion in mice. Taken together, compound **38** is a highly $G_{i/o}$-biased D_2R partial

agonist with the potential to serve as a tool compound for elucidating the role of G protein-mediated D_2R signaling in pathophysiological systems.

EXPERIMENTAL SECTION

Chemistry General Procedures.

High-performance liquid chromatography (HPLC) spectra for all compounds were acquired using an Agilent 1200 series system with a diode array detector. Chromatography was performed on a 2.1 × 150 mm^2 Zorbax 300SB-C18 5 μm column with water containing 0.1% formic acid as solvent A and acetonitrile containing 0.1% formic acid as solvent B at a flow rate of 0.4 mL/min. The gradient program was as follows: 1% B (0–1 min), 1–99% B (1–4 min), and 99% B (4–8 min). High-resolution mass spectra (HRMS) data were acquired in a positive ion mode using an Agilent G1969A API-TOF with an electrospray ionization (ESI) source. Nuclear magnetic resonance (NMR) spectra were acquired on either a Bruker DRX-600 spectrometer (600 MHz ^{1}H) or a Bruker Avance-III 800 MHz spectrometer (201 MHz ^{13}C). Chemical shifts are reported in ppm (δ). Preparative HPLC was performed on Agilent Prep 1200 series with UV detector set to 254 nm. Samples were injected into a Phenomenex Luna 250 × 30 mm^2, 5 μM C_{18} column at room temperature (rt). The flow rate was 40 mL/min. A linear gradient was used with 10% (or 50%) of MeOH (A) in H2O (with 0.1% TFA) (B) to 100% of MeOH (A). HPLC was used to establish the purity of target compounds. All final compounds had >95% purity using the HPLC methods described above. All final compounds are characterized as trifluoroacetic acid salt form, except compound **38**, of which form is free base.

Methyl *trans*-4-((*tert*-Butoxycarbonyl)amino)cyclohexane-1-carboxylate (1).

To a solution of 4-aminocyclohexane-1-carboxylic acid HCl salt (5 g, 27.9 mmol) in methanol (100 mL) was added thionyl chloride (7.5 mL, 103.5 mmol) at 0 °C. The resulting solution was warmed to rt and stirred for 18 h. Solvent removal under reduced pressure yielded the crude product as an off-white solid, which was used in the next step without further purification.

To a solution of the crude intermediate in dichloromethane (100 mL) was added triethylamine (6 mL, 43 mmol) at 0 °C, followed by di-*tert*-butyl dicarbonate (8.6 g, 39.5 mmol). The reaction was stirred overnight before being quenched with saturated aqueous sodium bicarbonate. The mixture was extracted with dichloromethane (3 × 50 mL). Combined organic phase was dried over anhydrous sodium sulfate and concentrated under reduced pressure. The resulting residue was purified by silica gel flash chromatography (elution with hexane/EtOAc = 1:1) to give compound **1** as white powder (6.84 g, 95%). ^{1}H NMR (600 MHz, CD_3OD) δ 3.67 (s, 3H), 3.33–3.25 (m, 1H), 2.36–2.16 (m, 1H), 2.03–1.88 (m, 4H), 1.45–1.47 (m, 11H), 1.31–1.16 (m, 2H).

tert-Butyl (*trans*-4-(Hydroxymethyl)cyclohexyl)carbamate (2).

To a solution of methyl *trans*-4-((*tert*-butoxycarbonyl)amino)cyclohexane-1-carboxylate (6.84, 26.5 mmol) in diethyl ether (120 mL) and methanol (0.6 mL) was added lithium borohydride (1.83 g, 84 mmol) in portions, followed by dropwise addition of methanol (3

mL). The resulting mixture was stirred for 45 min before being quenched with methanol and concentrated under reduced pressure. The resulting residue was treated with 1% aqueous sodium hydroxide and extracted with ethyl acetate (3 × 60 mL). The combined organic phase was dried over anhydrous sodium sulfate and concentrated under reduced pressure. The resulting residue was purified with silica gel flash chromatography (elution with MeOH/DCM = 0–10%) to give the title compound as white solid (5.8 g, 95%). ^{1}H NMR (600 MHz, CD_3OD) δ 3.37 (dd, J = 6.4, 1.3 Hz, 2H), 3.31–3.20 (m, 1H), 1.98–1.90 (m, 2H), 1.89–1.81 (m, 2H), 1.52–1.36 (m, 10H), 1.23–1.16 (m, 2H), 1.09–0.97 (m, 2H).

tert-Butyl (*trans*-4-(Cyanomethyl)cyclohexyl)carbamate (3).

To the solution of *tert*-butyl (*trans*-4-(hydroxymethyl)cyclohexyl)carbamate (4.34 g, 18.9 mmol) and triethylamine (5.3 mL, 37.8 mmol) in dichloromethane (150 mL) was added methanesulfonyl chloride (2.2 mL, 28.3 mmol) dropwise at 0 °C. The resulting mixture was stirred for 2 h before being quenched with water. The mixture was extracted with dichloromethane (3 × 60 mL). Combined organic phase was dried over sodium sulfate. After filtration, the solvent was removed under reduced pressure to provide the crude intermediate, which was used in next step without purification.

The crude material and potassium cyanide (3.6 g, 55.2 mmol) were mixed in dimethyl sulfoxide (60 mL). The mixture was stirred for 5 h at 100 °C, before being cooled to room temperature. After being cooled to rt, the reaction was diluted with water and extracted with ethyl acetate (3 × 100 mL). Combined organic phase was dried over sodium sulfate. The concentrated residue was purified by silica gel column (elution with hexane/EtOAc = 1:1) to yield the title compound as gray solid (4.3 g, 96%). ^{1}H NMR (600 MHz, CD_3OD) δ 3.32–3.25 (m, 1H), 2.40 (d, J = 6.5, 1.4 Hz, 2H), 1.96 (d, J = 10.4 Hz, 2H), 1.89 (d, J = 11.1 Hz, 2H), 1.69–1.58 (m, 1H), 1.45 (s, 9H), 1.28–1.09 (m, 4H).

tert-Butyl (*trans*-4-(2-Oxoethyl)cyclohexyl)carbamate (4).

To a solution of *tert*-butyl (*trans*-4-(hydroxymethyl)cyclohexyl)carbamate (1.2 g, 5 mmol) in dichloromethane (20 mL), was added diisobutylaluminium hydride (1 M in hexane, 15 mL) at −78 °C. The resulting solution was stirred for 2 h before being quenched with saturated aqueous solution of Rochelle's salt. The mixture was warmed to rt slowly and stirred vigorously until two phases were visualized. The organic phase was concentrated under reduced pressure. The resulting residue was purified by silica gel column to give the title compound as pale yellow solid (960 mg, 76%). ^{1}H NMR (600 MHz, $CDCl_3$) δ 9.75 (d, J = 2.3 Hz, 1H), 4.38 (s, 1H), 3.47–3.30 (m, 1H), 2.32 (dd, J = 6.8, 2.2 Hz, 2H), 2.00 (d, J = 10.7 Hz, 2H), 1.90–1.74 (m, 3H), 1.43 (s, 9H), 1.15–1.08 (m, 4H).

tert-Butyl (*cis*-4-(Hydroxymethyl)cyclohexyl)carbamate (6).

Compound **6** was prepared according to the same procedures as preparing compound **2** (yield 95%). ^{1}H NMR (600 MHz, CD_3OD) δ 3.56 (m, 1H), 3.43 (d, J = 6.4 Hz, 2H), 1.65–1.53 (m, 8H), 1.43 (s, 9H), 1.41–1.34 (m, 1H).

tert-Butyl (*cis*-4-(Cyanomethyl)cyclohexyl)carbamate (7).

Compound **7** was prepared according to the same procedures as preparing compound **3** (yield 96%). ^{1}H NMR (600 MHz, CD_3OD) δ 3.68–3.54 (m, 1H), 2.41 (dd, J = 7.2, 3.6 Hz, 2H), 1.83–1.55 (m, 9H), 1.44 (s, 9H).

tert-Butyl ((1*s*,4*s*)-4-(2-Oxoethyl)cyclohexyl)carbamate (8).

Compound **8** was prepared according to the same procedures as preparing compound **4** (yield 80%). ^{1}H NMR (600 MHz, $CDCl_3$) δ 9.75 (d, J = 2.2 Hz, 1H), 4.61 (s, 1H), 3.77–3.65 (m, 1H), 2.37 (dd, J = 6.9, 2.1 Hz, 2H), 2.12–1.97 (m, 1H), 1.66–1.56 (m, 6H), 1.44 (s, 9H), 1.29–1.18 (m, 2H).

3-(*trans*-4-(2-(4-(2,3-Dichlorophenyl)piperazin-1-yl)ethyl)cyclohexyl)-1,1-dimethylurea (9).

To the solution of Compound **11** (20 mg, 0.03 mmol) and triethylamine (12 mg, 0.12 mmol) in dichloromethane (2 mL) was added dimethylcarbamoyl chloride (7 mg, 0.06 mmol). The mixture was stirred for few minutes before being condensed. The resulting residue was purified by preparative HPLC (10–100% methanol/0.1% TFA in H_2O) to give the title compound as white powder (8 mg, 43%). ^{1}H NMR (600 MHz, CD_3OD) δ 7.37–7.29 (m, 2H), 7.24–7.18 (m, 1H), 3.73–3.67 (m, 2H), 3.603.46 (m, 3H), 3.36–3.24 (m, 4H), 3.18–3.04 (m, 2H), 2.90 (s, 6H), 1.97–1.91 (m, 2H), 1.92–1.84 (m, 2H), 1.77–1.66 (m, 2H), 1.43–1.25 (m, 3H), 1.17 (dd, J = 12.4, 3.5 Hz, 2H). MS (ESI) m/z 427.4 $[M + H]^+$.

tert-Butyl (*trans*-4-(2-(4-(2,3-Dichlorophenyl)piperazin-1-yl)ethyl)cyclohexyl)carbamate (10).

To a solution of 1-(2,3-dichlorophenyl)piperzine (46.2 mg, 0.2 mmol) and aldehyde **4** (48.2 mg, 0.2 mmol) in chloromethane (4 mL) was added sodium triacetoxyborohydride (84.8 mg, 0.4 mmol) in portions. The resulting mixture was stirred overnight before being quenched with saturated aqueous sodium bicarbonate. The resulting mixture was extracted with dichloromethane (3 × 10 mL). The combined organic phase was dried over sodium sulfate and concentrated under reduced pressure. The resulting residue was purified by preparative HPLC (10–100% methanol/0.1% TFA in H_2O) and lyophilized to give the title compounds as white powder (85.5 mg, yield 75%). ^{1}H NMR (600 MHz, CD_3OD) δ 7.36–7.30 (m, 2H), 7.20–7.16 (m, 1H), 3.73–3.68 (m, 2H), 3.59–3.52 (m, 2H), 3.36–3.25 (m, 5H), 3.21–3.09 (m, 2H), 1.99–1.91 (m, 2H), 1.89–1.82 (m, 2H), 1.77–1.67 (m, 2H), 1.46 (s, 9H), 1.39–1.32 (m, 1H), 1.27–1.09 (m, 4H). MS (ESI) m/z 456.7 $[M + H]^+$.

trans-4-(2-(4-(2,3-Dichlorophenyl)piperazin-1-yl)ethyl)-cyclohexan-1-amine (11).

Compound **10** (60 mg, 0.1 mmol) was treated with dichloromethane (1 mL) and trifluoroacetic acid (1 mL) for 1 h. After removal of the solvents, the resulting residue was purified by preparative HPLC (10–100% methanol/0.1% TFA in H_2O) to give the title compound as white powder (35.5 mg, 58%). ^{1}H NMR (600 MHz, CD_3OD) δ 7.37–7.29 (m, 2H), 7.18 (dd, J = 7.5, 2.1 Hz, 1H), 3.71 (d, J = 12.1 Hz, 2H), 3.56 (d, J = 13.2 Hz, 2H), 3.38–3.23 (m, 5H), 3.17–3.04 (m, 2H), 2.12–2.04 (m, 2H), 2.00–1.92 (m, 2H), 1.81–1.70 (m, 2H), 1.44 (qd, J = 12.5, 3.5 Hz, 3H), 1.25–1.18 (m, 2H). MS (ESI) m/z 356.2 $[M + H]^+$.

3-(*cis*-4-(2-(4-(2,3-Dichlorophenyl)piperazin-1-yl)ethyl)cyclohexyl)-1,1-dimethylurea (12).

To a solution of 1-(2,3-dichlorophenyl)piperzine (23.1 mg, 0.1 mmol) and compound 8 (24.1 mg, 0.1 mmol) in dichloromethane (2 mL) was added sodium triacetoxyborohydride (42.4 mg, 0.2 mmol) in portions. The resulting mixture was stirred overnight before being quenched with saturated aqueous sodium bicarbonate. The mixture was extracted with dichloromethane (3 × 5 mL). The combined organic phase was dried over sodium sulfate and concentrated under reduced pressure. The residue was treated with dichloromethane (1 mL) and trifluoroacetic acid (1 mL) for 1 h. After the solvent was removed under reduced pressure, the resulting residue was used in the next step without further purification. The crude material was dissolved in dichloromethane (2 mL). To the resulting solution was added triethylamine (50 mg, 0.5 mmol). After the solution was stirred for a few minutes, dimethylcarbamoyl chloride (22 mg, 0.2 mmol) in dichloromethane (1 mL) was added dropwise. After the resulting solution was stirred for 1 h, the mixture was concentrated under reduced pressure. The resulting residue was purified by preparative HPLC (10–100% methanol/0.1% TFA in H_2O) to give the title compound as white powder (25.3 mg, yield 47%). ^{1}H NMR (600 MHz, CD_3OD) δ 7.39–7.26 (m, 2H), 7.22–7.16 (m, 1H), 3.77–3.65 (m, 2H), 3.61–3.51 (m, 2H), 3.39–3.24 (m, 5H), 3.20–3.10 (m, 2H), 2.93 (s, 6H), 1.89–1.80 (m, 2H), 1.73–1.60 (m, 7H), 1.58–1.46 (m, 2H). MS (ESI) *m/z* 427.5 $[M + H]^+$.

3-(5-(4-(2,3-Dichlorophenyl)piperazin-1-yl)pentyl)-1,1-dimethylurea (15).

To a solution of **13** (203 mg, 1 mmol) and triethylamine (200 mg, 2 mmol) in dichloromethane (10 mL) was added methanesulfonyl chloride (137.4 mg, 1.2 mmol) dropwise at 0 °C. The resulting solution was stirred for 2 h at rt before being quenched with 1 mL of saturated aqueous sodium bicarbonate. The mixture was extracted with dichloromethane and washed with water. The organic phase was dried over anhydrous sodium sulfate, filtered, and concentrated under reduced pressure. The resulting residue was dissolved in acetonitrile (10 mL) before potassium carbonate (414.6 mg, 3 mmol) and 1-(2,3-dichlorophenyl)piperzine (231 mg, 1 mmol) were added successively. The mixture was refluxed overnight before being diluted with 10 mL of water. After being cooled to rt, the mixture was extracted with ethyl acetate (3 × 10 mL). The combined organic phase was dried over anhydrous sodium sulfate and concentrated under reduced pressure. The resulting residue was purified by silica gel column (CH_3OH/DCM, 0–10%) to give compound **14** (50 mg, yield 12%). Compound **14** was treated with trifluoroacetic acid (1 mL) and dichloromethane (2 mL) for 3 h at rt. The reaction was condensed under reduced pressure. The resulting residue was used for next step without further purification. To a solution of the residue above and triethylamine (40 mg, 0.4 mmol) in dichloromethane (2 mL), was added dimethylcarbamoyl chloride (16.1 mg, 0.15 mmol). The mixture was stirred for 1 h before being concentrated under reduced pressure. The resulting residue was purified by preparative HPLC (10–100% methanol/0.1% TFA in H_2O) to give the title compound as a white powder (20 mg, yield 33%). ^{1}H NMR (600 MHz, CD_3OD) δ 7.40–7.25 (m, 2H), 7.24–7.17 (m, 1H), 3.71 (d, J = 12.1 Hz, 2H), 3.55 (d, J = 13.1 Hz, 2H), 3.36–3.28 (m, 2H), 3.27–3.23 (m, 2H), 3.22–3.13 (m, 4H), 2.91 (s, 6H), 1.89–1.80 (m, 2H), 1.65–1.53 (m, 2H), 1.45 (t, J = 7.3 Hz, 2H). MS (ESI) *m/z* 387.4 $[M + H]^+$.

General Procedure for Preparing 16–19, 21–25.

Compound **20** (212 mg, 0.45 mmol) was treated with trifluoroacetic acid (10 mL) and dichloromethane (10 mL) for 3 h at rt. The solution was concentrated under reduced pressure. The resulting residue was dissolved in dichloromethane (9 mL). To the solution was added triethylamine (404 mg, 4.0 mmol). The mixture was equally divided into nine portions. To each portion was added the corresponding acyl chloride or anhydride (0.1 mmol, 2 equiv). The resulting mixture was stirred overnight, followed by concentration under reduced pressure. The resulting residue was purified by preparative HPLC (10–100% methanol/0.1% TFA in H_2O) to give the title compound as a white powder.

3-(*trans*-4-(2-(3,4-Dihydroisoquinolin-2(1*H*)-yl)ethyl)cyclohexyl)-1,1-dimethylurea (16).

Dimethylcarbamoyl chloride was used to afford a powder (15 mg, yield 68%). ^{1}H NMR (600 MHz, CD_3OD) δ 7.38–7.26 (m, 3H), 7.23 (d, J = 7.5 Hz, 1H), 4.62 (d, J = 15.3 Hz, 1H), 4.34 (d, J = 15.3 Hz, 1H), 3.89–3.79 (m, 1H), 3.56–3.47 (m, 1H), 3.44–3.23 (m, 4H), 3.19–3.12 (m, 1H), 2.92–2.84 (m, 6H), 1.96–1.91 (m, 2H), 1.90–1.83 (m, 2H), 1.81–1.73 (m, 2H), 1.43–1.38 (m, 1H), 1.36–1.27 (m, 2H), 1.22–1.12 (m, 2H). MS (ESI) *m/z* 330.8 $[M + H]^+$.

3-(*trans*-4-(2-(3,4-Dihydroisoquinolin-2(1*H*)-yl)ethyl)cyclohexyl)-1,1-diethylurea (17).

Diethylcarbamoyl chloride was used to afford a powder (yield 54%). ^{1}H NMR (600 MHz, CD_3OD) δ 7.35–7.26 (m, 3H), 7.23–7.19 (m, 1H), 4.69–4.27 (m, 2H), 3.88–3.48 (m, 3H), 3.38–3.31 (m, 8H), 1.96–1.89 (m, 2H), 1.85 (d, J = 12.5 Hz, 2H), 1.79–1.70 (m, 2H), 1.42–1.25 (m, 3H), 1.22–1.05 (m, 8H). MS (ESI) *m/z* 358.4 $[M + H]^+$.

3-(*trans*-4-(2-(3,4-Dihydroisoquinolin-2(1*H*)-yl)ethyl)cyclohexyl)-1,1-diisopropylurea (18).

Diisopropylcarbamoyl chloride was used to afford a powder (yield 60%). ^{1}H NMR (600 MHz, CD_3OD) δ 7.34–7.25 (m, 3H), 7.21 (d, J = 7.4 Hz, 1H), 4.65–4.51 (m, 2H), 3.81–3.73 (m, 2H), 3.57–3.42 (m, 3H), 3.41–3.26 (m, 2H), 3.24–3.10 (m, 2H), 1.93 (d, J = 12.2 Hz, 2H), 1.88–1.81 (m, 2H), 1.80–1.68 (m, 2H), 1.43–1.34 (m, 1H), 1.34–1.06 (m, 16H). MS (ESI) *m/z* 386.8 $[M + H]^+$.

N-(*trans*-4-(2-(3,4-Dihydroisoquinolin-2(1*H*)-yl)ethyl)cyclohexyl)pyrrolidine-1-carboxamide (19).

Pyrrolidine-1-carbonyl chloride was used to afford a powder (yield 39%). ^{1}H NMR (600 MHz, CD_3OD) δ 7.38–7.24 (m, 3H), 7.24–7.19 (m, 1H), 4.70–4.27 (m, 2H), 3.90–3.49 (m, 3H), 3.46–3.39 (m, 4H), 3.25–3.06 (m, 4H), 2.01–1.81 (m, 8H), 1.78–1.72 (m, 2H), 1.45–1.35 (m, 1H), 1.33–1.26 (m, 2H), 1.24–1.13 (m, 2H). MS (ESI) *m/z* $[M + H]^+$.

tert-Butyl (*trans*-4-(2-(3,4-Dihydroisoquinolin-2(1*H*)-yl)ethyl)cyclohexyl)carbamate (20).

Compound **20** was prepared by the same procedures as preparing compound **10**. 1,2,3,4-Tetrahydroisoquinoline (266 mg, 2 mmol), compound **4** (482 mg, 2 mmol) and sodium triacetoxyborohydride (848 mg, 4 mmol) were used to give the title compound as an oil (460 mg, yield 49%). ^{1}H NMR (600 MHz, CD_3OD) δ 7.40–7.14 (m, 4H), 4.62 (d, J = 15.0 Hz,

1H), 4.34 (d, J = 15.1 Hz, 1H), 3.94–3.62 (m, 3H), 3.43–2.98 (m, 4H), 2.13–1.63 (m, 6H), 1.48–1.28 (m, 10H), 1.27–1.06 (m, 4H). MS (ESI) *m/z* 359.9 $[M + H]^+$.

Isopropyl (*trans*-4-(2-(3,4-Dihydroisoquinolin-2(1*H*)-yl)ethyl)cyclohexyl)carbamate (21).

Isopropyl chloroformate was used to afford a powder (yield 74%). ^{1}H NMR (600 MHz, CD_3OD) δ 7.34–7.24 (m, 3H), 7.21 (d, J = 7.6 Hz, 1H), 4.57–4.32 (m, 2H), 3.74–3.40 (m, 3H), 3.37–3.28 (m, 3H), 3.23–3.12 (m, 2H), 1.94 (d, J = 12.5 Hz, 2H), 1.85 (d, J = 12.8 Hz, 2H), 1.79–1.71 (m, 2H), 1.42–1.33 (m, 1H), 1.31–1.07 (m, 10H). MS (ESI) *m/z* 345.5 $[M + H]^+$.

Ethyl (*trans*-4-(2-(3,4-Dihydroisoquinolin-2(1*H*)-yl)ethyl)cyclohexyl)carbamate (22).

Ethyl chloroformate was used to afford a powder (yield 41%). ^{1}H NMR (600 MHz, CD_3OD) δ 7.35–7.23 (m, 3H), 7.21 (d, J = 7.6 Hz, 1H), 4.67–4.24 (m, 2H), 4.10–3.98 (m, 2H), 3.93–3.55 (m, 3H), 3.48–3.09 (m, 4H), 1.94 (d, J = 12.3 Hz, 2H), 1.87 (dd, J = 27.4, 13.1 Hz, 2H), 1.80–1.70 (m, 2H), 1.43–1.36 (m, 2H), 1.29–1.07 (m, 6H). MS (ESI) *m/z* 331.7 $[M + H]^+$.

N-(*trans*-4-(2-(3,4-Dihydroisoquinolin-2(1*H*)-yl)ethyl)cyclohexyl)benzamide (23).

Benzoyl chloride was used to afford a powder (yield 59%). ^{1}H NMR (600 MHz, CD_3OD) δ 7.82–7.77 (m, 2H), 7.54–7.49 (m, 1H), 7.44 (dd, J = 8.4, 7.0 Hz, 2H), 7.35–7.26 (m, 3H), 7.22 (d, J = 7.2 Hz, 1H), 4.64–4.58 (m, 1H), 4.36–4.30 (m, 1H), 3.90–3.77 (m, 1H), 3.43–3.21 (m, 5H), 3.17 (s, 1H), 2.06–1.99 (m, 2H), 1.91 (d, J = 13.1 Hz, 2H), 1.84–1.74 (m, 2H), 1.47–1.40 (m, 3H), 1.28–1.18 (m, 2H). MS (ESI) *m/z* 363.5 $[M + H]^+$.

N-(*trans*-4-(2-(3,4-Dihydroisoquinolin-2(1*H*)-yl)ethyl)cyclohexyl)propionamide (24).

Propionyl chloride was used to afford a powder (yield 74%). ^{1}H NMR (600 MHz, CD_3OD) δ 7.34–7.26 (m, 3H), 7.23–7.17 (m, 1H), 4.78–4.42 (m, 2H), 3.70–3.54 (m, 3H), 3.42–3.30 (m, 2H), 3.24–3.14 (m, 2H), 2.16 (q, J = 7.5 Hz, 2H), 1.92 (d, J = 12.2 Hz, 2H), 1.86 (d, J = 12.6 Hz, 2H), 1.78–1.72 (m, 2H), 1.41–1.35 (m, 1H), 1.34–1.15 (m, 4H), 1.11 (t, J = 7.7 Hz, 3H). MS (ESI) *m/z* 315.3 $[M + H]^+$.

N-(*trans*-4-(2-(3,4-Dihydroisoquinolin-2(1*H*)-yl)ethyl)cyclohexyl)acetamide (25).

Acetic anhydride was used to afford a powder (yield 58%). ^{1}H NMR (600 MHz, CD_3OD) δ 7.35–7.23 (m, 3H), 7.21 (d, J = 7.5 Hz, 1H), 4.65–4.26 (m, 2H), 3.84–3.43 (m, 3H), 3.36–3.29 (m, 2H), 3.24–3.13 (m, 2H), 1.96–1.89 (m, 5H), 1.88–1.81 (m, 2H), 1.79–1.69 (m, 2H), 1.43–1.33 (m, 1H), 1.28–1.12 (m, 4H). MS (ESI) *m/z* 301.4 $[M + H]^+$.

3-(*cis*-4-(2-(3,4-Dihydroisoquinolin-2(1*H*)-yl)ethyl)cyclohexyl)-1,1-dimethylurea (26).

Compound **26** (21 mg, yield 64%) was prepared using the same procedures as preparing compound **16**–**19** and **21**–**25** from 1,2,3,4-tetrahydroisoquinoline (13.3 mg, 0.1 mmol), compound **4** (24.1 mg, 0.1 mmol) and sodium triacetoxyborohydride (42.4 mg, 0.2 mmol). ^{1}H NMR (600 MHz, CD_3OD) δ 7.37–7.27 (m, 3H), 7.26–7.20 (m, 1H), 4.64 (d, J = 15.1 Hz, 1H), 4.36 (d, J = 15.1 Hz, 1H), 3.87–3.83 (m, 1H), 3.75–3.67 (m, 1H), 3.46–3.39 (m, 1H), 3.36–3.26 (m, 3H), 3.21–3.12 (m, 1H), 2.93 (s, 6H), 1.89 (t, J = 7.1 Hz, 2H), 1.74–1.59 (m, 7H), 1.59–1.45 (m, 2H). MS (ESI) *m/z* 330.8 $[M + H]^+$.

tert-Butyl (*trans*-4-((3,4-Dihydroisoquinolin-2(1*H*)-yl)methyl)cyclohexyl)carbamate (27).

Compound **27** (31 mg, yield 15%) was prepared using the same procedures as preparing compound **14** from 1,2,3,4-tetrahydroisoquinoline (133 mg, 1 mmol) and compound **6** (100 mg, 0.44 mmol). ^{1}H NMR (600 MHz, CD_3OD) δ 7.34–7.22 (m, 3H), 7.21 (dd, J = 7.5, 1.4 Hz, 1H), 4.59 (d, J = 15.4 Hz, 1H), 4.32 (d, J = 15.3 Hz, 1H), 3.93–3.69 (m, 1H), 3.43–3.34 (m, 1H), 3.30 (d, J = 1.6 Hz, 3H), 3.19–3.08 (m, 2H), 2.01–1.82 (m, 5H), 1.43 (s, 9H), 1.34–1.25 (m, 2H), 1.24–1.12 (m, 2H). MS (ESI) *m/z* 345.6 $[M + H]^+$.

3-(*trans*-4-((3,4-Dihydroisoquinolin-2(1*H*)-yl)methyl)cyclohexyl)-1,1-dimethylurea (28).

Compound **28** (15 mg, yield 68%) was prepared using the same procedures as preparing compound **15** from compound **27** (31 mg, 0.07 mmol). ^{1}H NMR (600 MHz, CD_3OD) δ 7.33–7.25 (m, 3H), 7.21 (d, J = 7.5 Hz, 1H), 4.64–4.54 (m, 1H), 4.37–4.29 (m, 1H), 3.87–3.75 (m, 1H), 3.56–3.48 (m, 1H), 3.44–3.36 (m, 1H), 3.32–3.24 (m, 2H), 3.19–3.10 (m, 2H), 2.88 (s, 6H), 2.01–1.84 (m, 5H), 1.43–1.33 (m, 2H), 1.26–1.14 (m, 2H). MS (ESI) *m/z* 316.6 $[M + H]^+$.

3-(4-(2-(3,4-Dihydroisoquinolin-2(1*H*)-yl)ethyl)phenyl)-1,1-dimethylurea (30).

To a solution of compound **29** (40 mg, 0.16 mmol) and triethylamine (32 mg, 0.32 mmol) in dichloromethane (5 mL) was added methanesulfonyl chloride (22.8 mg, 0.2 mmol) dropwise at 0 °C. The solution was stirred for 2 h at rt before being quenched with saturated aqueous sodium bicarbonate. The mixture was diluted with water and extracted with dichloromethane. The organic phase was dried over anhydrous sodium sulfate and concentrated under reduced pressure. The resulting rESIdue was dissolved in acetonitrile (5 mL). To the resulting solution were added potassium carbonate (69 mg, 0.5 mmol) and 1,2,3,4-tetrahydroisoquinoline (65 mg, 0.5 mmol). The mixture was refluxed overnight before being diluted with water (10 mL) and extracted with ethyl acetate (3 × 10 mL). The organic phase was dried over anhydrous sodium sulfate and concentrated under reduce pressure. The resulting rESIdue was purified by silica gel column (CH3OH/DCM, 0–10%) to give an oil intermediate (30 mg). The intermediate was treated with trifluoroacetic acid (1 mL) and dichloromethane (2 mL) for 3 h at rt before being condensed under reduced pressure. To a mixture of the resulting rESIdue and potassium carbonate (40 mg, 0.3 mmol) in tetrahydrofuran (2 mL) was added dimethylcarbamoyl chloride (16.1 mg, 0.2 mmol). The mixture was stirred for 1 h before being condensed under reduced pressure. The resulting rESIdue was purified by preparative HPLC (10–100% methanol/0.1% TFA in H_2O) to give the title compound as white powder (17 mg, yield 23%). ^{1}H NMR (600 MHz, CD_3OD) δ 7.37 (d, J = 8.2 Hz, 2H), 7.35–7.26 (m, 3H), 7.23 (dd, J = 12.3, 7.8 Hz, 3H), 4.51 (d, J = 105.7 Hz, 2H), 3.99–3.64 (m, 1H), 3.54–3.44 (m, 3H), 3.27–3.17 (m, 2H), 3.12 (dd, J = 10.4, 6.3 Hz, 2H), 3.01 (s, 6H). MS (ESI) *m/z* 324.3 $[M + H]^+$.

3-(5-(3,4-Dihydroisoquinolin-2(1*H*)-yl)pentyl)-1,1-dimethylurea (32).

Compound **32** (40 mg, yield 10%) was prepared using the same procedures as preparing compound **15** from 1,2,3,4-tetrahydroisoquinoline (133 mg, 1 mmol). ^{1}H NMR (600 MHz, CD_3OD) δ 7.34–7.24 (m, 3H), 7.21 (d, J = 7.5 Hz, 1H), 4.44 (s, 2H), 3.61–3.55 (m, 2H),

3.28–3.24 (m, 2H), 3.23–3.17 (m, 4H), 2.87 (s, 6H), 1.89–1.83 (m, 2H), 1.63–1.55 (m, 2H), 1.47–1.42 (m, 2H). MS (ESI) *m/z* 290.3 $[M + H]^+$.

3-(*trans*-4-(2-(5,6-Dichloro-3,4-dihydroisoquinolin-2(1*H*)-yl)ethyl)cyclohexyl)-1,1-dimethylurea (33).

Compound **33** (27 mg, 53%) was prepared using the same procedures as preparing compound **12** from 5,6-dichloro-1,2,3,4-tetrahydroisoquinoline (20.2 mg, 0.1 mmol) and compound **4** (24.1 mg, 0.1 mmol). ^{1}H NMR (600 MHz, CD_3OD) δ 7.51 (d, J = 8.3 Hz, 1H), 7.21 (d, J = 8.4 Hz, 1H), 4.64–4.30 (m, 2H), 3.83–3.45 (m, 3H), 3.37–3.32 (m, 2H), 3.26–3.17 (m, 2H), 2.87 (s, 6H), 1.92 (dd, J = 13.4, 3.7 Hz, 2H), 1.85 (d, J = 12.5 Hz, 2H), 1.78–1.71 (m, 2H), 1.42–1.35 (m, 1H), 1.34–1.29 (m, 2H), 1.19–1.12 (m, 2H). MS (ESI) *m/z* 398.1 $[M + H]^+$.

3-(*trans*-4-(2-(7,8-Dihydro-[1,3]dioxolo[4,5-*g*]isoquinolin-6(5*H*)-yl)ethyl)cyclohexyl)-1,1-dimethylurea (34).

Compound **34** (24 mg, 49%) was prepared using the same procedures as preparing compound **12** from 5,6,7,8-tetrahydro-[1,3]dioxolo[4,5-*g*]isoquinoline (17.7 mg, 0.1 mmol) and compound 4 (24.1 mg, 0.1 mmol). ^{1}H NMR (600 MHz, CD_3OD) δ 6.72 (s, 1H), 6.67 (s, 1H), 5.95 (s, 2H), 4.52–4.39 (m, 1H), 4.25–4.12 (m, 1H), 3.82–3.67 (m, 1H), 3.51–3.45 (m, 1H), 3.35–3.26 (m, 3H), 3.17–2.98 (m, 2H), 2.87 (s, 6H), 1.92 (dd, J = 13.5, 3.8 Hz, 2H), 1.87–1.81 (m, 2H), 1.76–1.71 (m, 2H), 1.39–1.33 (m, 1H), 1.34–1.26 (m, 2H), 1.18–1.09 (m, 2H). MS (ESI) *m/z* 374.2 $[M + H]^+$.

3-(*trans*-4-(2-(5-Chloro-3,4-dihydroisoquinolin-2(1*H*)-yl)ethyl)cyclohexyl)-1,1-dimethylurea (35).

Compound **35** (23 mg, 48%) was prepared using the same procedures as preparing compound **12** from 5-chloro-1,2,3,4-tetrahydroisoquinoline (13.3 mg, 0.1 mmol) and compound 4 (24.1 mg, 0.1 mmol). ^{1}H NMR (600 MHz, CD_3OD) δ 7.43 (d, J = 7.9 Hz, 1H), 7.34–7.29 (m, 1H), 7.20 (d, J = 7.7 Hz, 1H), 4.64–4.28 (m, 2H), 3.87–3.45 (m, 3H), 3.35–3.29 (m, 2H), 3.20–3.13 (m, 2H), 2.87 (s, 6H), 1.94–1.89 (m, 2H), 1.85 (d, J = 13.1 Hz, 2H), 1.78–1.72 (m, 2H), 1.43–1.35 (m, 1H), 1.33–1.27 (m, 2H), 1.19–1.12 (m, 2H). MS (ESI) *m/z* 364.2 $[M + H]^+$.

3-(*trans*-4-(2-(6-Chloro-3,4-dihydroisoquinolin-2(1*H*)-yl)ethyl)cyclohexyl)-1,1-dimethylurea (36).

Compound **36** (19 mg, 40%) was prepared using the same procedures as preparing compound **12** from 6-chloro-1,2,3,4-tetrahydroisoquinoline (13.3 mg, 0.1 mmol) and compound **4** (24.1 mg, 0.1 mmol). ^{1}H NMR (600 MHz, CD_3OD) δ 7.32 (dd, J = 8.3, 2.2 Hz, 1H), 7.29–7.25 (m, 2H), 4.71–4.13 (m, 2H), 3.92–3.41 (m, 3H), 3.34–3.30 (m, 2H), 3.24–3.10 (m, 2H), 2.87 (s, 6H), 1.94–1.89 (m, 2H), 1.85 (d, J = 12.5 Hz, 2H), 1.77–1.72 (m, 2H), 1.42–1.35 (m, 1H), 1.34–1.26 (m, 2H), 1.17–1.12 (m, 2H). MS (ESI) *m/z* 364.2 $[M + H]^+$.

3-(*trans*-4-(2-(7-Chloro-3,4-dihydroisoquinolin-2(1*H*)-yl)ethyl)cyclohexyl)-1,1-dimethylurea (37).

Compound **37** (19 mg, 42%) was prepared using the same procedures as preparing compound **12** from 7-chloro-1,2,3,4-tetrahydroisoquinoline (13.3 mg, 0.1 mmol) and compound **4** (24.1 mg, 0.1 mmol). ^{1}H NMR (600 MHz, CD_3OD) δ 7.35–7.29 (m, 2H), 7.21 (dd, J = 8.4, 1.8 Hz, 1H), 4.56–4.31 (m, 2H), 3.79–3.44 (m, 3H), 3.34–3.27 (m, 2H), 3.23–3.11 (m, 2H), 2.87 (s, 6H), 1.92–1.93 (m, 2H), 1.85 (d, J = 13.1 Hz, 2H), 1.77–1.69 (m, 2H), 1.42–1.35 (m, 1H), 1.34–1.25 (m, 2H), 1.18–1.12 (m, 2H). MS (ESI) *m/z* 364.1 $[M + H]^+$.

3-(*trans*-4-(2-(8-Chloro-3,4-dihydroisoquinolin-2(1*H*)-yl)ethyl)cyclohexyl)-1,1-dimethylurea (38).

Compound **38** (25 mg, 52%) was prepared using the same procedures as preparing compound **12** from 8-chloro-1,2,3,4-tetrahydroisoquinoline (13.3 mg, 0.1 mmol) and compound **4** (24.1 mg, 0.1 mmol). A portion of compound **38** was converted to free base form with aqueous sodium bicarbonate for ^{1}H NMR and ^{13}C NMR. ^{1}H NMR (800 MHz, CD_3OD) δ 7.22 (d, J = 7.9 Hz, 1H), 7.19–7.15 (m, 1H), 7.10 (d, J = 7.6 Hz, 1H), 3.66 (s, 2H), 3.56–3.49 (m, 1H), 2.95 (t, J = 6.1 Hz, 2H), 2.89 (s, 6H), 2.76 (t, J = 6.0 Hz, 2H), 2.66–2.61 (m, 2H), 1.93 (dd, J = 13.1, 4.0 Hz, 2H), 1.89–1.84 (m, 2H), 1.59–1.53 (m, 2H), 1.36–1.29 (m, 3H), 1.12 (dd, J = 12.3, 3.3 Hz, 2H). ^{13}C NMR (201 MHz, CD_3OD) δ 159.1, 136.7, 131.9, 131.8, 127.1, 127.1, 126.2, 56.0, 53.6, 50.0, 49.7, 35.4, 35.1, 33.4, 33.0, 32.1, 28.5. MS (ESI) *m/z* 364.2 $[M + H]^+$. HRMS *m/z* $[M + H]^+$ calcd for $C_{20}H_{31}ClN_3O_+$ 364.2150, found 364.2165.

1,1-Dimethyl-3-(*trans*-4-(2-(8-methyl-3,4-dihydroisoquinolin-2(1*H*)-yl)ethyl)cyclohexyl)urea (39).

Compound **39** (19 mg, 42%) was prepared using the same procedures as preparing compound **12** from 8-methyl-1,2,3,4-tetrahydroisoquinoline (14.7 mg, 0.1 mmol) and compound **8** (24.1 mg, 0.1 mmol). ^{1}H NMR (600 MHz, CD_3OD) δ 7.22–7.16 (m, 1H), 7.10 (dd, J = 17.3, 7.5 Hz, 2H), 4.55 (d, J = 15.5 Hz, 1H), 4.20 (d, J = 15.5 Hz, 1H), 3.80 (d, J = 11.1 Hz, 1H), 3.54–3.46 (m, 1H), 3.44–3.20 (m, 4H), 3.10 (d, J = 16.5 Hz, 1H), 2.87 (s, 6H), 2.27 (s, 3H), 1.98–1.89 (m, 2H), 1.86 (d, J = 13.1 Hz, 2H), 1.81–1.75 (m, 2H), 1.43–1.35 (m, 1H), 1.34–1.26 (m, 2H), 1.21–1.09 (m, 2H). MS (ESI) *m/z* 344.2 $[M + H]^+$.

3-(*trans*-4-(2-(8-Bromo-3,4-dihydroisoquinolin-2(1*H*)-yl)ethyl)cyclohexyl)-1,1-dimethylurea (40).

Compound **40** (24 mg, 46%) was prepared using the same procedures as preparing compound **12** from 8-bromo-1,2,3,4-tetrahydroisoquinoline (21.2 mg, 0.1 mmol) and compound **4** (24.1 mg, 0.1 mmol). ^{1}H NMR (600 MHz, CD_3OD) δ 7.56 (d, J = 7.8 Hz, 1H), 7.30 (d, J = 7.7 Hz, 1H), 7.25 (t, J = 7.8 Hz, 1H), 4.64–4.18 (m, 2H), 3.85–3.44 (m, 3H), 3.42–3.37 (m, 2H), 3.26–3.20 (m, 2H), 2.87 (s, 6H), 1.92 (dd, J = 13.4, 3.7 Hz, 2H), 1.86 (d, J = 12.3 Hz, 2H), 1.77 (q, J = 7.4 Hz, 2H), 1.43–1.36 (m, 1H), 1.35–1.28 (m, 2H), 1.19–1.13 (m, 2H). MS (ESI) *m/z* 408.2 $[M + H]^+$.

3-(*trans*-4-(2-(8-Fluoro-3,4-dihydroisoquinolin-2(1*H*)-yl)ethyl)cyclohexyl)-1,1-dimethylurea (41).

Compound **41** (20 mg, 43%) was prepared using the same procedures as preparing compound **12** from 8-fluoro-1,2,3,4-tetrahydroisoquinoline (15.1 mg, 0.1 mmol) and compound **4** (24.1 mg, 0.1 mmol). ^{1}H NMR (600 MHz, CD_3OD) δ 7.39–7.34 (m, 1H), 7.11 (d, J = 7.8 Hz, 1H), 7.06 (dd, J = 9.9, 8.3 Hz, 1H), 4.33 (s, 2H), 3.85–3.44 (m, 3H), 3.40–3.35 (m, 2H), 3.27–3.19 (m, 2H), 2.87 (s, 6H), 1.93–1.89 (m, 2H), 1.88–1.82 (m, 2H), 1.80–1.73 (m, 2H), 1.43–1.35 (m, 1H), 1.34–1.26 (m, 2H), 1.19–1.12 (m, 2H). MS (ESI) *m/z* 348.2 $[M + H]^+$.

1,1-Dimethyl-3-(*trans*-4-(2-(8-(trifluoromethyl)-3,4-dihydroisoquinolin-2(1*H*)-yl)ethyl)cyclohexyl)urea (42).

Compound **42** (15 mg, 29%) was prepared using the same procedures as preparing compound **12** from 8-(trifluoromethyl)-1,2,3,4-tetrahydroisoquinoline (15.1 mg, 0.1 mmol) and compound **4** (24.1 mg, 0.1 mmol). ^{1}H NMR (600 MHz, CD_3OD) δ 7.68 (d, J = 7.6 Hz, 1H), 7.57 (d, J = 7.7 Hz, 1H), 7.54–7.49 (m, 1H), 4.78–4.42 (m, 2H), 4.03–3.69 (m, 1H), 3.53–3.46 (m, 1H), 3.45–3.28 (m, 5H), 2.87 (s, 6H), 1.95–1.89 (m, 2H), 1.88–1.83 (m, 2H), 1.81–1.69 (m, 2H), 1.44–1.35 (m, 1H), 1.34–1.24 (m, 2H), 1.19–1.10 (m, 2H). MS (ESI) *m/z* 398.2 $[M + H]^+$.

3-(*trans*-4-(2-(8-Methoxy-3,4-dihydroisoquinolin-2(1*H*)-yl)ethyl)cyclohexyl)-1,1-dimethylurea (43).

Compound **43** (19 mg, 40%) was prepared using the same procedures as preparing compound **12** from 8-methoxy-1,2,3,4-tetrahydroisoquinoline (16.3 mg, 0.1 mmol) and compound **4** (24.1 mg, 0.1 mmol). ^{12}H NMR (600 MHz, CD_3OD) δ 7.12 (d, J = 8.5 Hz, 1H), 6.88–6.82 (m, 1H), 6.81 (d, J = 2.6 Hz, 1H), 4.59–4.17 (m, 2H), 3.78 (s, 3H), 3.53–3.34 (m, 1H), 3.33–3.24 (m, 4H), 3.23–3.11 (m, 2H), 2.87 (d, J = 1.3 Hz, 6h), 1.92 (dd, J = 12.9, 3.7 Hz, 2H), 1.87–1.82 (m, 2H), 1.76–1.70 (m, 2H), 1.42–1.34 (m, 1H), 1.34–1.23 (m, 2H), 1.19–1.06 (m, 2H). MS (ESI) *m/z* 360.4 $[M + H]^+$.

Experimental Procedures for in Vitro Biochemical Assays.

D_2R $G_{i/O}$-Mediated cAMP Inhibition Assay.—D_2R or D^3R $G_{i/o}$-mediated cAMP inhibition assays were performed in parallel with D_2R or D_3R β-Arrestin recruitment Tango assays. Human D_2R or D_3R transfected HEK293T cells co-expressing the cAMP biosensor GloSensor-22F (Promega) were seeded (15 000 cells/40 μL/well) into white 384 clear-bottom, tissue culture plates in Dulbecco's modified Eagle's medium (DMEM) containing 1% dialyzed fetal bovine serum (FBS). Next day, drug dilutions were made in drug buffer (Hank's balanced salt solution (HBSS), 20 mM *N*-(2-hydroxyethyl)piperazine-*N*-ethanesulfonic acid (HEPES), 0.1% bovine serum albumin (BSA), 0.01% ascorbic acid, pH 7.4), and the same drug dilutions used for the $G_{i/o}$-mediated cAMP inhibition assays were also used for β-arrestin recruitment Tango assay. Media were removed and 20 μL of drug buffer was added per well and allowed to equilibrate for at least 15 min room temperature. To start the assay, cells were treated with 5 μL/well of 5× drug using a FLIPR (Molecular Devices). After 15 min, cAMP accumulation was initiated by the addition of 5 μL/well of

either 0.3 μM isoproterenol (final concentration) for D_2R or 1 μM of Forskolin for D_3R diluted in GloSensor reagent. Luminescence per well per second was read on a MicroBeta plate counter (PerkinElmer). Data were normalized to maximum cAMP inhibition by quinpirole (100%) and basal cAMP accumulation by isoproterenol (0%). Data were analyzed using the sigmoidal dose–response function built into GraphPad Prism 5.0. Notably, HEK293T cells expressing the GloSensor-22F alone (no hD_2R) were assayed in parallel and displayed no inhibition of isoproterenol-stimulated cAMP, either by quinpirole or by the test compounds, suggesting that the effect observed in hD_{2L}-expressing cells was due to compound acting via the recombinant receptor.

D_2R β-Arrestin Recruitment Tango Assay.—Recruitment of β-arrestin to agonist-stimulated D_{2L} or D_3 receptors was performed using Tango.[41,56] Briefly, HTLA cells stably expressing β-arrestin-TEV protease and a tetracycline transactivator-driven luciferase were plated in 15 cm dishes in DMEM containing 10% FBS and transfected (via calcium phosphate) with 10 μg of a D_2V_2-TCS-tTA or D_3V_2-TCS-tTA construct. The next day, cells were plated in white, clear-bottom, 384-well plates (Greiner; 15 000 cells/well, 40 μL/well) in DMEM containing 1% dialyzed FBS. The following day, media were decanted and exchanged for fresh DMEM media containing 1% dialyzed FBS. Importantly, the same drug dilutions used for the $G_{i/o}$-mediated cAMP inhibition assay were used for the Tango assay to prevent compound solubility variability between assays. Cells were treated with 10 μL/well of drug using a FLIPR and for D_2R antagonist assays, antagonists were diluted in 10 nM dopamine. After at least 20–22 h, the medium were removed and replaced with 1:20 diluted BrightGlo reagent (Promega), and luminescence per well was read using a MicroBeta plate counter (PerkinElmer). Data were normalized to vehicle (0%) and quinpirole or dopamine-stimulated controls (100%) and analyzed using the sigmoidal dose–response function built into GraphPad Prism 5.0.

D_2R β-Arrestin Recruitment BRET Assay.—To measure D_2R-mediated β-arrestin recruitment, HEK293T cells were co-transfected in a 1:1:15 ratio with human D_{2long} containing a C-terminal renilla luciferase (RLuc8), GRK2, and Venus-tagged N-terminal β-arrestin2. Next day, transfected cells were plated in polylysine coated 96-well white clear-bottom cell culture plates in plating media (DMEM +1% dialyzed FBS) at a density of 30 000–40 000 cells in 200 μL/well and incubated overnight. Next day, media was decanted and cells were washed twice with 60 μL of drug buffer (1× HBSS, 20 mM HEPES, 0.1% BSA, 0.01% ascorbic acid, pH 7.4). Then 60 μL of drug buffer was added per well and drug stimulation was initiated with addition of 30 μL of drug (3×) per well. Then 10 μL/well of RLuc substrate, coelenterazine h (Promega, 5 μM final concentration) was added and read 15 min post drug addition, which is the same time point for D_2R Gαi1-γ2 dissociation BRET assay. Plates were read for both luminescence at 485 nm and fluorescent eYFP emission at 530 nm for 1 s/well using a Mithras LB940. The ratio of eYFP/RLuc was calculated per well and the net BRET ratio was calculated by subtracting the eYFP/RLuc per well from the eYFP/RLuc ratio in wells without Venus-β-arrestin2 present. The net BRET ratio was plotted as a function of drug concentration using GraphPad Prism 5 (GraphPad Software Inc., San Diego, CA). Data were normalized to % quinpirole or dopamine stimulation and analyzed using nonlinear regression log(agonist) versus response.

D_2R Gαi1-γ2 Dissociation BRET Assay.—To measure D_2R-mediated Gαi1-γ2 dissociation, HEK293T cells were co-transfected in a 1:1:1:1 ratio of Gαi1-RLuc, Gβ1, GFP_2-Gγ2, and human D_{2long}, respectively. Gαi1-RLuc, Gβ1, and Gγ2-GFP_2 constructs were generously provided by Dr. Michel Bouvier. Cells were plated and assays were performed exactly similar to the BRET arrestin assay, except the substrate used was Coelenterazine 400a (NanoLight, 5 μM final concentration). Plates were read after 15 min drug incubation, which is the same time point for D_2R β-arrestin recruitment BRET assay, measuring luminescence at 400 nm and fluorescent GFP_2 emission at 515 nm for 1 s/well using a Mithras LB940. The ratio of GFP_2/RLuc was calculated per well and plotted as a function of drug concentration using GraphPad Prism 5 (GraphPad Software Inc., San Diego, CA). Data were normalized to % quinpirole stimulation and analyzed using nonlinear regression log(agonist) versus response.

Bias Calculation.—Transduction coefficients (log(τ/K_A)) were calculated using the Black and Leff operational model in GraphPad Prism 5.0, where τ is agonist efficacy and K_A is the equilibrium dissociation constant and were calculated with respect to quinpirole, the D2 full agonist reference. Transduction coefficients were calculated for both pathways and averaged across experiments. Calculation of bias factors utilized the method by Kenakin et al.,[57] where the $\Delta\log/\tau K_A$) was calculated relative to the reference and the $\Delta\Delta\log(\tau/K_A.)$ was calculated by subtracting the β-arrestin2 from the $G_{i/o}$ transduction coefficient to yield the antilog transformed bias factors with respect to $G_{i/o}$ activity.

Molecular Docking of Compounds 1, 16, and 38.—The crystal structure of the dopamine D_2 receptor (D_2R) in complex with risperidone was retrieved from the Protein Data Bank (www.rcsb.org) by its identifying code (PDB: 6CM4). The structure was then manually edited to remove the T4 lysozyme, oleic acid, and the di(hydroxyethyl)ether. The structure also contained three thermo-stabilizing mutations: I122$^{3.40}$A, L375$^{6.37}$A, and L379$^{6.41}$A, which were retained, as these rESIdue positions are not near the ligand binding site and were not predicted to impact binding pose. Risperidone was retained for purposes of maintaining an orthosteric site that was conducive to ligand binding during the modeling process. Because antagonists, such as risperidone, are known to stabilize different receptor conformations compared to agonists, we sought to compare this structure to that of a previous D_2R model that was successfully implemented to model functionally selective D_2 agonists.[41] The two structures were aligned and superimposed in PyMol 2.2.0. The allatom binding site root-mean-square deviation (RMSD) was computed in PyMol after overlaying the two D_2R structures and selecting the atoms in the transmembrane helices and extracellular domains that border the orthosteric binding pocket of the receptor. The RMSD was calculated to ensure sufficient similarity between the atom positions of the rESIdues important for binding. The all-atom binding site RMSD between our model and this previous D_2R model was 0.74 Å,[41] which indicates a high degree of similarity between the arrangements of the atoms lining the binding pockets of both structures (Figure 3A). Compounds **1**, **16**, and **38** were docked to the orthosteric binding site of our D_2R model using DOCK3.7.2.[58] As previously described,[59] the Dock 3.7.2 program superimposes atoms of each molecule onto matching spheres to dock flexible ligands into a binding site. Matching spheres represent favorable positions for individual ligand atoms, and in this study,

45 was used, based on the atom positions of the original risperidone complex. For docking, the receptor structure was prepared, and AMBER united-atom charges were assigned. Reduce[60] was utilized to protonate receptor structures, whereas partial charges from the united-atom AMBER[61] force field were used for all receptor atoms. Energy grids were used to assess the various energy terms of the DOCK scoring function including AMBER van der Waals potential, Poisson–Boltzmann electrostatic potentials using QNIFFT, and ligand desolvation from the occluded volume of the target for different ligand orientations. Prior to docking, ligand conformations and protonation states were calculated, and ligands were prepared in an energy-minimized state. Marvin (version 18.12, ChemAxon, 2018; https://www.chemaxon.com) was used to protonate each ligand at pH 7.4. Corina[62] (Molecular Networks GmbH) was then used to create a three-dimensional rendering of each protomer before conformational sampling via Omega (OpenEye Scientific Software).[63] Finally, AMSOL[64] was used to compute the charges and initial solvation energies of the ligands. Following docking to the matching spheres, the lowest energy poses for each ligand were visualized and compared with existing crystal structures of ligands bound to aminergic GPCRs.[38,65,66]

Experimental Procedures for in Vivo Studies in Mice.

Receptor Occupancy Assay.—In vivo receptor occupancy was assessed in male c57 mice. All procedures performed on animals were in accordance with regulations and established guidelines and were reviewed and approved by an Institutional Animal Care and Use Committee.

Mice were dosed with vehicle (5% DMSO: 5% Cremophor: 90% saline plus 1 mequiv of HCl) or **38** (0.32, 1, 3.2, 10, or 32 mg/kg) subcutaneously at a dose volume of 10 mL/kg. After 20 min of the subcutaneous dose, the mice were dosed retro-orbitally with 100 μci [^{3}H]raclopride at a dose volume of 5 mL/kg. After a 30 min drug pretreatment period, the animals were euthanized by live decapitation. Trunk blood was collected and centrifuged at 7500 rpm for 10 min, and the plasma was collected and stored at −80 °C until exposure level analysis. The striatum and the cerebellum (used to define nonspecific binding) were immediately dissected and homogenized in 20 mg/mL of assay buffer (20 mM HEPES, 4.16 mM $NaHCO_3$, 0.44 mM KH_2PO_4, 0.63 mM NaH_2PO_4 127 mM NaCl, 5.36 mM KCl, 1.26 mM $CaCl_2$, 0.98 mM $MgCl_2$) with a polytron for 10 s. The rest of the brain was immediately frozen on dry ice and stored at −80 °C until exposure level analysis. Striatum or cerebellum (400 μL) was filtered through presoaked Whatman GF/B filter circles followed by 2 × 5 mL of assay buffer. Filters were transferred to scintillation vials containing Ultima Gold MV scintillation cocktail. Radioactivity was measured using the PerkinElmer TriCarb liquid scintillation counter.

Locomotor Activity Assay.—Adult male and female C57BL/6 mice were housed 3–5/cage on a 14:10 h light/dark cycle (lights on 0700 h) in a humidity- and temperature-controlled room with food and water provided ad libitum. All experiments were conducted with an approved protocol from the Duke University Institutional Animal Care and Use Committee. Motor activity was assessed in a 21 × 21 × 30 cm^3 open field (Omnitech Inc., Columbus, OH) under 340 lx illumination. C57BL/6 mice were housed in the test room 24 h

prior to testing. Animals were injected (i.p.) with vehicle or different doses of **38** and immediately placed into the open field. After 30 min, mice were removed from the test arena and given (i.p.) the vehicle or 6 mg/kg PCP (Sigma-Aldrich, St. Louis, MO) and returned immediately to the open field for an additional 90 min. Horizontal distance traveled (cm) was quantitated with Fusion software (Omnitech) and scored in 5 min bins across testing. The behavioral data are presented as means and standard errors of the mean and analyzed by repeated measures ANOVA followed by Bonferroni-corrected pair-wise comparisons where a $p < 0.05$ was considered significant.

Supplementary Material

Refer to Web version on PubMed Central for supplementary material.

ACKNOWLEDGMENTS

The research described here was supported in part by the grant U19MH082441 (to J.J. and B.L.R.) from the U.S. National Institutes of Health. J.J. and B.L.R. acknowledge the support by the grant U24DK116195 from the U.S. National Institutes of Health. J.J. also acknowledges the support by the grant R01NS100930 from the U.S. National Institutes of Health. M.L.M. acknowledges the support by the NIGMS-funded Integrated Pharmacological Sciences Training Program T32 GM062754 and the MSTP training grants at the Icahn School of Mount Sinai (NIH T32 GM007280). We thank Dr. Xufen Yu for detailedly reading synthetic procedures and characterization data. We thank Drs. Brian K. Shoichet and Isha Singh for strictly reading molecular docking method and Dr. Xin Chen for helpful discussions.

ABBREVIATIONS

GPCR	G protein-coupled receptor
SFSR	structure—functional selectivity relationships
D_2R	dopamine D_2 receptor
cAMP	cyclic adenosine monophosphate
LHS	left-hand side
RHS	right-hand side
BRET	bioluminescence resonance energy transfer
GRK2	G protein-coupled receptor kinase 2
D_1R	dopamine D_1 receptor
D_3R	dopamine D_3 receptor
D_4R	dopamine D_4 receptor
D_4R	dopamine D_5 receptor
TFA	trifluoroacetic acid
DCM	dichloromethane

REFERENCES

(1). Wacker D; Stevens RC; Roth BL How ligands illuminate GPCR molecular pharmacology. Cell 2017, 170, 414–427. [PubMed: 28753422]

(2). Roth BL; Sheffler DJ; Kroeze WK Magic shotguns versus magic bullets: selectively non-selective drugs for mood disorders and schizophrenia. Nat. Rev. Drug Discovery 2004, 3, 353–359. [PubMed: 15060530]

(3). Vallano A; Fernandez-Duenas V; Pedros C; Arnau JM; Ciruela F An update on adenosine A2A receptors as drug target in Parkinson's disease. CNS Neurol. Disord.: Drug Targets 2011, 10, 659–669. [PubMed: 21838670]

(4). Fan X; Xu M; Hess EJ D_2 dopamine receptor subtype- mediated hyperactivity and amphetamine responses in a model of ADHD. Neurobiol. Dis. 2010, 37, 228–236. [PubMed: 19840852]

(5). Reimann F; Gribble FM G protein-coupled receptors as new therapeutic targets for type 2 diabetes. Diabetologia 2016, 59, 229–233. [PubMed: 26661410]

(6). Hauser AS; Chavali S; Masuho I; Jahn LJ; Martemyanov KA; Gloriam DE; Babu MM Pharmacogenomics of GPCR drug targets. Cell 2018, 172, 41–54. [PubMed: 29249361]

(7). Roth BL; Irwin JJ; Shoichet BK Discovery of new GPCR ligands to illuminate new biology. Nat. Chem. Biol. 2017, 13, 1143–1151. [PubMed: 29045379]

(8). Furchgott RF The Use of Haloalkylamines in the Differentiation of Receptors and in the Determination of Dissociation Constants of Agonist-Receptor Complexes In Advances in Drug Research; Harper N, Simmonds A, Eds.; Academic Press: New York, 1966; Vol. 3, pp 21–55.

(9). Chang SD; Bruchas MR Functional selectivity at GPCRs: new opportunities in psychiatric drug discovery. Neuropsychopharmacology 2014, 39, 248–249. [PubMed: 24317323]

(10). Kenakin T Functional selectivity and biased receptor signaling. J. Pharmacol. Exp. Ther. 2011, 336, 296–302. [PubMed: 21030484]

(11). Peters MF; Scott CW Evaluating cellular impedance assays for detection of GPCR pleiotropic signaling and functional selectivity. J. Biomol Screen. 2009, 14, 246–255. [PubMed: 19211780]

(12). Tan L; Yan W; McCorvy JD; Cheng J Biased ligands of G protein-coupled receptors (GPCRs): structure-functional selectivity relationships (SFSRs) and therapeutic potential. J. Med. Chem. 2018, 61, 9841–9878. [PubMed: 29939744]

(13). Urban JD; Clarke WP; von Zastrow M; Nichols DE; Kobilka B; Weinstein H; Javitch JA; Roth BL; Christopoulos A; Sexton PM; Miller KJ; Spedding M; Mailman RB Functional selectivity and classical concepts of quantitative pharmacology. J. Pharmacol. Exp. Ther. 2007, 320, 1–13. [PubMed: 16803859]

(14). Kenakin T; Christopoulos A Signalling bias in new drug discovery: detection, quantification and therapeutic impact. Nat. Rev. Drug Discovery 2013, 12, 205–216. [PubMed: 23411724]

(15). Rajagopal K; Lefkowitz RJ; Rockman HA When 7 transmembrane receptors are not G protein-coupled receptors. J. Clin. Invest. 2005, 115, 2971–2974. [PubMed: 16276410]

(16). Rajagopal K; Whalen EJ; Violin JD; Stiber JA; Rosenberg PB; Premont RT; Coffman TM; Rockman HA; Lefkowitz RJ Beta-arrestin2-mediated inotropic effects of the angiotensin II type 1A receptor in isolated cardiac myocytes. Proc. Natl. Acad. Sci U.SA. 2006, 103, 16284–16289.

(17). Bohn LM; Gainetdinov RR; Lin FT; Lefkowitz RJ; Caron MG Mu-opioid receptor desensitization by beta-arrestin-2 determines morphine tolerance but not dependence. Nature 2000, 408, 720–723. [PubMed: 11130073]

(18). Metra M; Cas LD; di Lenarda A; Poole-Wilson P Beta-blockers in heart failure: are pharmacological differences clinically important? Heart Fail. Rev. 2004, 9, 123–130. [PubMed: 15516860]

(19). Wisler JW; DeWire SM; Whalen EJ; Violin JD; Drake MT; Ahn S; Shenoy SK; Lefkowitz RJ A unique mechanism of beta-blocker action: Carvedilol stimulates beta-arrestin signaling. Proc. Natl. Acad. Sci. U.S.A. 2007, 104, 16657–16662. [PubMed: 17925438]

(20). Manglik A; Lin H; Aryal DK; McCorvy JD; Dengler D; Corder G; Levit A; Kling RC; Bernat V; Hubner H; Huang XP; Sassano MF; Giguere PM; Lober S; Da D; Scherrer G; Kobilka BK; Gmeiner P; Roth BL; Shoichet BK Structure-based discovery of opioid analgESIcs with reduced side effects. Nature 2016, 537, 185–190. [PubMed: 27533032]

(21). Kilts JD; Connery HS; Arrington EG; Lewis MM; Lawler CP; Oxford GS; O'Malley KL; Todd RD; Blake BL ; Nichols DE; Mailman RB Functional selectivity of dopamine receptor agonists. II. Actions of dihydrexidine in D_2L receptor- transfected MN9D cells and pituitary lactotrophs. J. Pharmacol. Exp. Ther. 2002, 301, 1179–1189. [PubMed: 12023553]

(22). Mailman RB GPCR functional selectivity has therapeutic impact. Trends Pharmacol. Sci. 2007, 28, 390–396. [PubMed: 17629962]

(23). Urban JD; Vargas GA; von Zastrow M; Mailman RB Aripiprazole has functionally selective actions at dopamine D_2 receptor-mediated signaling pathways. Neuropsychopharmacology 2007, 32, 67–77. [PubMed: 16554739]

(24). Violin JD; Lefkowitz RJ Beta-arrestin-biased ligands at seven-transmembrane receptors. Trends Pharmacol. Sci. 2007, 28, 416–422. [PubMed: 17644195]

(25). Gesty-Palmer D; Flannery P; Yuan L; Corsino L; Spurney R; Lefkowitz RJ; Luttrell LM A beta-arrestin-biased agonist of the parathyroid hormone receptor (PTH1R) promotes bone formation independent of G protein activation. Sci. Transl. Med. 2009, 1, No. 1ra1.

(26). Butini S; Gemma S; Campiani G; Franceschini S; Trotta F; Borriello M; Ceres N; Ros S; Coccone SS; Bernetti M; De Angelis M; Brindisi M; Nacci V; Fiorini I; Novellino E; Cagnotto A; Mennini T; Sandager-Nielsen K; Andreasen JT; Scheel-Kruger J; Mikkelsen JD; Fattorusso C Discovery of a new class of potential multifunctional atypical antipsychotic agents targeting dopamine D_3 and serotonin 5-HT1A and 5-HT2A receptors: dESIgn, synthESIs, and effects on behavior. J. Med. Chem. 2009, 52, 151–169. [PubMed: 19072656]

(27). Shonberg J; Herenbrink CK; Lopez L; Christopoulos A; Scammells PJ; Capuano B; Lane JR A structure-activity analysis of biased agonism at the dopamine D_2 receptor. J. Med. Chem. 2013, 56, 9199–9221. [PubMed: 24138311]

(28). Hiller C; Kling RC; Heinemann FW; Meyer K; Hubner H; Gmeiner P Functionally selective dopamine D_2/D_3 receptor agonists comprising an enyne moiety. J. Med. Chem. 2013, 56, 5130–5141. [PubMed: 23730937]

(29). Szabo M; Klein Herenbrink C; Christopoulos A; Lane JR; Capuano B Structure-activity relationships of privileged structures lead to the discovery of novel biased ligands at the dopamine D(2) receptor. J. Med. Chem. 2014, 57, 4924–4939. [PubMed: 24827597]

(30). Möler D; Kling RC; Skultety M; Leuner K; Hübner H; Gmeiner P Functionally selective dopamine D(2), D(3) receptor partial agonists. J. Med. Chem. 2014, 57, 4861–4875. [PubMed: 24831693]

(31). Möller D; Banerjee A; Uzuneser TC; Skultety M; Huth T; Plouffe B; Hübner H; Alzheimer C; Friedland K; Muller CP; Bouvier M; Gmeiner P Discovery of G protein-biased dopaminergics with a pyrazolo[1,5-a]pyridine substructure. J. Med. Chem. 2017, 60, 2908–2929. [PubMed: 28248104]

(32). Männel B; Dengler D; Shonberg J; Hübner H; Möller D; Gmeiner P Hydroxy-substituted heteroarylpiperazines: novel scaffolds for beta-arrestin-biased D_2R agonists. J. Med. Chem. 2017, 60, 4693–4713. [PubMed: 28489379]

(33). Männel B; Jaiteh M; Zeifman A; Randakova A; Möller D; Hübner H; Gmeiner P; Carlsson J Structure-guided screening for functionally selective D_2 dopamine receptor ligands from a virtual chemical library. ACS Chem. Biol. 2017, 12, 2652–2661. [PubMed: 28846380]

(34). Männel B; Hübner H; Möller D; Gmeiner P Beta-arrestin biased dopamine D_2 receptor partial agonists: Synthesis and pharmacological evaluation. Bioorg. Med. Chem. 2017, 25, 5613–5628. [PubMed: 28870802]

(35). Allen JA; Yost JM; Setola V; Chen X; Sassano MF; Chen M; Peterson S; Yadav PN; Huang XP; Feng B; Jensen NH; Che X; Bai X; Frye SV; Wetsel WC; Caron MG; Javitch JA; Roth BL; Jin J Discovery of beta-arrestin-biased dopamine D_2 ligands for probing signal transduction pathways essential for antipsychotic efficacy. Proc. Natl. Acad. Sci. U.S.A. 2011, 108, 18488–18493. [PubMed: 22025698]

(36). Bonifazi A; Yano H; Guerrero AM; Kumar V; Hoffman AF; Lupica CR; Shi L; Newman AH Novel and potent dopamine D_2 receptor Go-protein biased agonists. ACS Pharmacol. Transl. Sci. 2019, 2, 52–65. [PubMed: 30775693]

(37). Beaulieu JM; Gainetdinov RR The physiology, signaling, and pharmacology of dopamine receptors. Pharmacol. Rev. 2011, 63, 182–217. [PubMed: 21303898]

(38). Wang S; Che T; Levit A; Shoichet BK; Wacker D; Roth AL Structure of the D_2 dopamine receptor bound to the atypical antipsychotic drug risperidone. Nature 2018, 555, 269–273. [PubMed: 29466326]

(39). Chen X; Sassano MF; Zheng L; Setola V; Chen M; Bai X ; Frye SV; Wetsel WC; Roth BL; Jin J Structure-functional selectivity relationship studies of beta-arrestin-biased dopamine D(2) receptor agonists. J. Med. Chem. 2012, 55, 7141–7153. [PubMed: 22845053]

(40). Chen X; McCorvy JD; Fischer MG; Butler KV; Shen Y ; Roth BL; Jin J Discovery of G protein-biased D_2 dopamine receptor partial agonists. J. Med. Chem. 2016, 59, 10601–10618. [PubMed: 27805392]

(41). McCorvy JD; Butler KV; Kelly B; Rechsteiner K; Karpiak J; Betz RM; Kormos BL; Shoichet BK; Dror RO; Jin J; Roth BL Structure-inspired dESIgn of beta-arrestin-biased ligands for aminergic GPCRs. Nat. Chem. Biol. 2018, 14, 126–134. [PubMed: 29227473]

(42). Javitch JA The ants go marching two by two: oligomeric structure of G-protein-coupled receptors. Mol. Pharmacol. 2004, 66, 1077–1082. [PubMed: 15319448]

(43). Mottola DM Functional selectivity of dopamine receptor agonists. I. Selective activation of postsynaptic dopamine D_2 receptors linked to adenylate cyclase. J. Pharmacol. Exp. Ther. 2002, 301, 1166–1178. [PubMed: 12023552]

(44). Tschammer N; Bollinger S; Kenakin T; Gmeiner P Histidine 6.55 is a major determinant of ligand-biased signaling in dopamine D_2L receptor. Mol. Pharmacol. 2011, 79, 575–585. [PubMed: 21163968]

(45). Free RB; Chun LS; Moritz AE; Miller BN; Doyle TB; Conroy JL; Padron A; Meade JA; Xiao J; Hu X; Dulcey AE; Han Y; Duan L; Titus S; Bryant-Genevier M; Barnaeva E; Ferrer M; Javitch JA; Beuming T; Shi L; Southall NT; Marugan JJ; Sibley DR Discovery and characterization of a G protein-biased agonist that inhibits beta-arrestin recruitment to the D_2 dopamine receptor. Mol. Pharmacol. 2014, 86, 96–105. [PubMed: 24755247]

(46). Kehr J; Yoshitake T; Ichinose F; Yoshitake S; Kiss B; Gyertyan I; Adham N Effects of cariprazine on extracellular levels of glutamate, GABA, dopamine, noradrenaline and serotonin in the medial prefrontal cortex in the rat phencyclidine model of schizophrenia studied by microdialysis and simultaneous recordings of locomotor activity. Psychopharmacology 2018, 235, 1593–1607. [PubMed: 29637288]

(47). Campbell RH; Diduch M; Gardner KN; Thomas C Review of cariprazine in management of psychiatric illness. Ment. Health Clin. 2017, 7, 221–229. [PubMed: 29955527]

(48). Kroeze WK; Sassano MF; Huang X-P; Lansu K; McCorvy JD; Giguere PM; Sciaky N; Roth BL PRESTO- Tango as an open-source resource for interrogation of the druggable human GPCRome. Nat. Struct. Mol. Biol. 2015, 22, 362–369. [PubMed: 25895059]

(49). Stemp G; Ashmeade T; Branch CL; Hadley MS; Hunter AJ; Johnson CN; Nash DJ; Thewlis KM; Vong AKK; Austin NE; Jeffrey P; Avenell KY; Boyfield I; Hagan JJ; Middlemiss DN; Reavill C; Riley GJ; Routledge C; Wood M Design and synthesis of trans-N-[4-[2-(6-cyano-1,2,3,4-tetrahydroi-soquinolin-2-yl)ethyl]cyclohexyl]-4-quinolinecarboxamide (SB- 277011): A potent and selective dopamine D_3 receptor antagonist with high oral bioavailability and CNS penetration in the rat. J. Med. Chem. 2000, 43, 1878–1885. [PubMed: 10794704]

(50). Klein Herenbrink C; Sykes DA; Donthamsetti P; Canals M; Coudrat T; Shonberg J; Scammells PJ; Capuano B; Sexton PM; Charlton SJ; Javitch JA; Christopoulos A; Lane JR The role of kinetic context in apparent biased agonism at GPCRs. Nat. Commun. 2016, 7, No. 10842.

(51). Masri B; Salahpour A; Didriksen M; Ghisi V; Beaulieu JM; Gainetdinov RR; Caron MG Antagonism of dopamine D_2 receptor/beta-arrestin 2 interaction is a common property of clinically effective antipsychotics. Proc. Natl. Acad. Sci. U.S.A. 2008, 105, 13656–13661. [PubMed: 18768802]

(52). Masuho I; Martemyanov KA; Lambert NA Monitoring G protein activation in cells with BRET In G Protein-Coupled Receptors in Drug Discovery; Filizola M, Ed.; Methods in Molecular Biology; Humana Press: NY, 2015; Vol. 1335, pp 107–113.

(53). Chun LS; Vekariya RH; Free RB; Li Y; Lin DT; Su P; Liu F; Namkung Y; Laporte SA; Moritz AE; Aube J; Frankowski KJ; Sibley DR Structure-activity investigation of a G protein-biased agonist reveals molecular determinants for biased signaling of the D_2 dopamine receptor. Front. Synaptic Neurosci. 2018, 10, No. 2.

(54). McCorvy JD; Wacker D; Wang S; Agegnehu B; Liu J; Lansu K; Tribo AR; Olsen RHJ; Che T; Jin J; Roth BL Structural determinants of 5-HT2B receptor activation and biased agonism. Nat. Struct. Mol. Biol. 2018, 25, 787–796. [PubMed: 30127358]

(55). Fell MJ; Perry KW; Falcone JF; Johnson BG; Barth VN ; Rash KS; Lucaites VL; Threlkeld PG; Monn JA; McKinzie DL; Marek GJ; Svensson KA; Nelson DL In vitro and in vivo evidence for a lack of interaction with dopamine D_2 receptors by the metabotropic glutamate 2/3 receptor agonists 1S,2S,5R,6S-2-aminobicyclo [3.1.0]hexane-2,6-bicaroxylate monohydrate (LY354740) and (−)-2-oxa-4-aminobicyclo[3.1.0] Hexane-4,6-dicarboxylic acid (LY379268). J. Pharmacol. Exp. Ther. 2009, 33, 1126–1136.

(56). Kroeze WK; Sassano MF; Huang XP; Lansu K; McCorvy JD; Giguere PM; Sciaky N; Roth BL PRESTO-Tango as an open-source resource for interrogation of the druggable human GPCRome. Nat. Struct. Mol. Biol. 2015, 22, 362–369. [PubMed: 25895059]

(57). Kenakin T; Watson C; Muniz-Medina V; Christopoulos A; Novick S A simple method for quantifying functional selectivity and agonist bias. ACS Chem. Neurosci. 2012, 3, 193–203. [PubMed: 22860188]

(58). Coleman RG; Carchia M; Sterling T; Irwin JJ; Shoichet BK Ligand pose and orientational sampling in molecular docking. PLoS One 2013, 8, No. e75992.

(59). Weiss DR; Ahn S; Sassano MF; Kleist A; Zhu X; Strachan R; Roth BL; Lefkowitz RJ; Shoichet BK Conformation guides molecular efficacy in docking screens of activated beta-2 adrenergic G protein coupled receptor. ACS Chem. Biol. 2013, 8, 1018–1026. [PubMed: 23485065]

(60). Word JM; Lovell SC; Richardson JS; Richardson DC Asparagine and glutamine: using hydrogen atom contacts in the choice of side-chain amide orientation. J. Mol. Biol. 1999, 285, 1735–1747. [PubMed: 9917408]

(61). Case DA; Berryman JT; Betz RM; Cerutti DS; Cheatham TE III; Darden TA; Duke RE; Giese TJ; Gohlke H; Goetz AW; Homeyer N; Izadi S; Janowski P; Kaus J; Kovalenko A; Lee TS; LeGrand S; Li P; Luchko T; Luo R; Madej B; Merz KM; Monard G; Needham P; Nguyen H; Nguyen HT; Omelyan I; Onufriev A; Roe DR; Roitberg A; Salomon-Ferrer R; Simmerling CL; Smith W; Swails J; Walker RC; Wang J; Wolf RM; Wu X; York DM; Kollman PA AMBER 2015; University of California: San Francisco, CA, 2015.

(62). Sadowski J; Gasteiger J; Klebe G Comparison of automatic three-dimensional model builders using 639 X-ray structures. J. Chem. Inf. Model. 1994, 34, 1000–1008.

(63). Hawkins PC; Skillman AG; Warren GL; Ellingson BA; Stahl MT Conformer generation with OMEGA: algorithm and validation using high quality structures from the Protein Databank and Cambridge Structural Database. J. Chem. Inf. Model. 2010, 50, 572–584. [PubMed: 20235588]

(64). Chambers CC; Hawkins GD; Cramer CJ; Truhlar DG Model for aqueous solvation based on class IV atomic charges and first solvation shell effects. J. Phys. Chem. 1996, 100, 16385–16398.

(65). Chien EY; Liu W; Zhao Q; Katritch V; Han GW; Hanson MA; Shi L; Newman AH; Javitch JA; Cherezov V; Stevens RC Structure of the human dopamine D_3 receptor in complex with a D_2/D_3 selective antagonist. Science 2010, 330, 1091–1095. [PubMed: 21097933]

(66). Wang S; Wacker D; Levit A; Che T; Betz RM; McCorvy JD; Venkatakrishnan AJ; Huang XP; Dror RO; Shoichet BK ; Roth BL D_4 dopamine receptor high-resolution structures enable the discovery of selective agonists. Science 2017, 358, 381–386. [PubMed: 29051383]

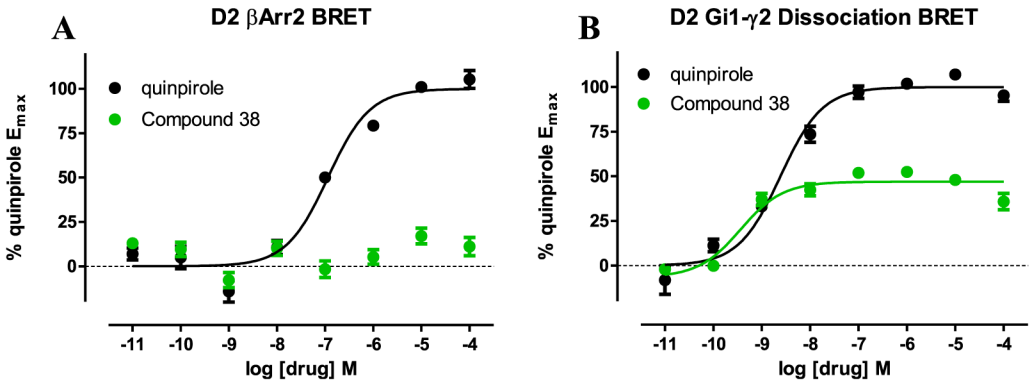

Figure 1.

Further confirmation that compound **38** is a G protein-biased D_2R partial agonist. (A) D_2R-mediated BRET β-arrestin recruitment activity of compounds **38** and quinpirole (EC_{50} = 115 nM). (B) D_2R-mediated Gi1 BRET activity of compounds **38** ($EC5_0$ = 0.37 nM, E_{max} = 47%) and quinpirole (EC_{50} = 2.4 nM). Data are the average of at least three independent experiments performed in duplicate.

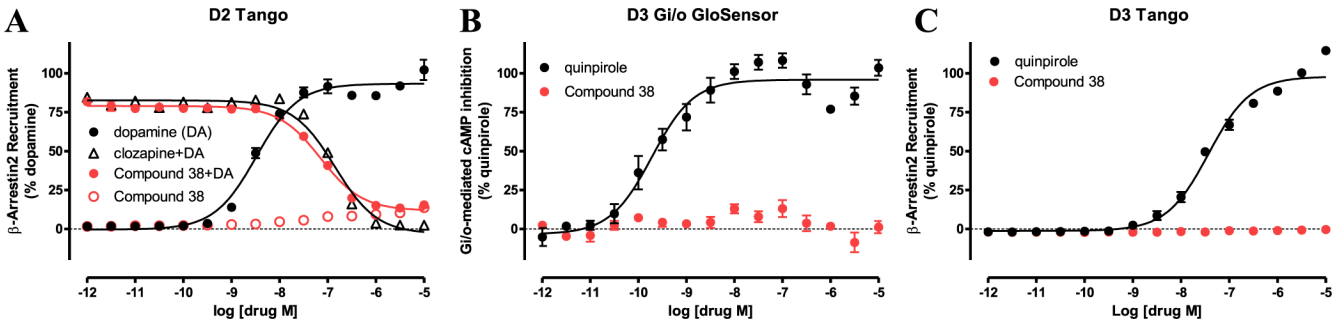

Figure 2.

(A) Antagonist activity of compound **38** (IC_{50} = 71 nM) on dopamine (DA)-stimulated D_2R *β*-arrestin recruitment is similar to clozapine (IC_{50} = 140 nM) as measured by Tango. Lack of D_3R agonist activity of compound **38** compared to positive control quinpirole in the $G_{i/o}$-mediated cAMP inhibition GloSensor assay (B) and *β*-arrestin recruitment Tango assay (C). Data are the average of three independent experiments performed in triplicate.

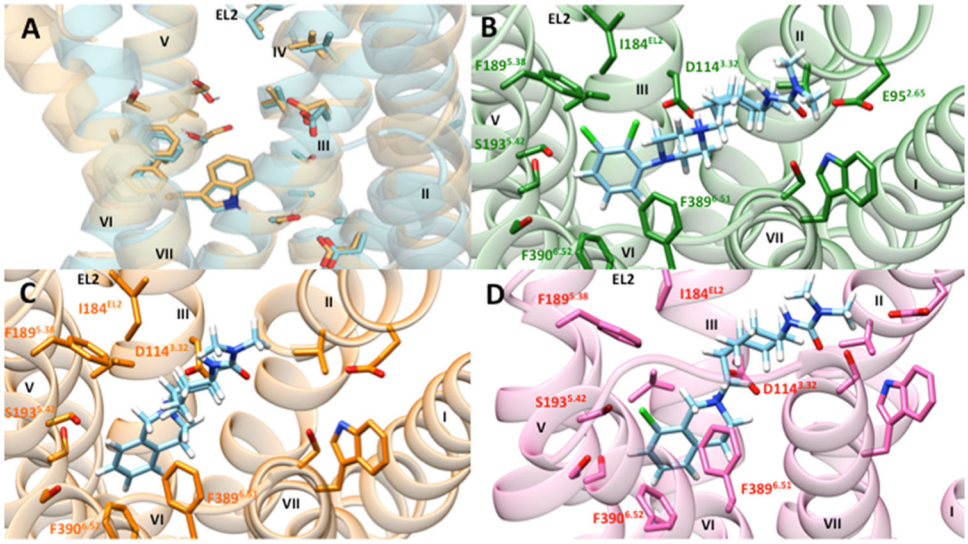

Figure 3.

In silico structure-based SFSR studies of D_2R agonists. (A) When the D_2R crystal structure utilized for this study (gold) is overlayed with a D_2R homology model from a previous study that examined the structural determinants of D_2R agonist functional selectivity (blue), a high degree of similarity was noted between the two structures (all-atom binding site RMSD = 0.74 Å).[41] (B) The docked pose of cariprazine suggests that together with $I184^{EL2}$, $F189^{5.38}$ may function as a "lid" over the binding pocket leading to increase ligand rESIdence times and *β*-arrestin recruitment. (C) Compound **16** engages D_2R from deeper within the orthosteric site, and the steric constraints it imposes on TM5 may partially underlie its $G_{i/o}$ bias. (D) Compound **38**'s chloro substituent forms a hydrogen bond with conserved TM5 serines and angles with the rest of the scaffold away from extracellular loop 2 (EL2), which would be predicted to enhance its G_i bias compared to **16**.

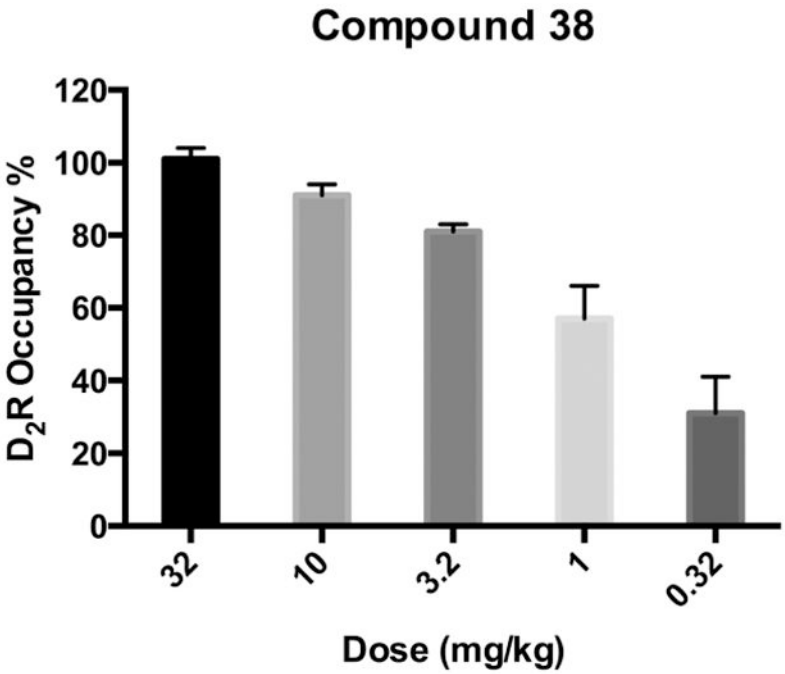

Figure 4.

Compound **38** exhibits dose dependence to binding to D_2 receptor in male c57 mice. [^{3}H]Raclopride in vivo binding assay was used.

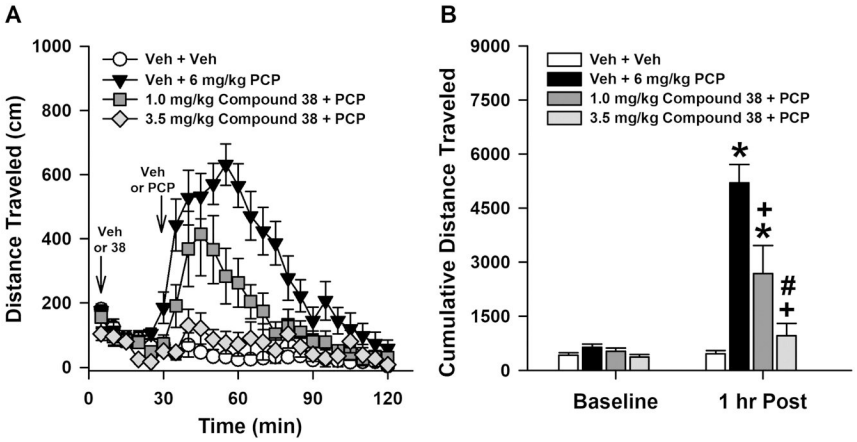

Figure 5.

Compound **38** displays a potent antipsychotic-like activity in a hyperlocomotion study. C57Bl/6 mice were given the vehicle (Veh), 1, or 3.5 mg/kg **38** (intraperitoneally (i.p.)), followed 30 min later with the Veh or 6 mg/kg phencyclidine (PCP, i.p.). (A) Locomotor activities are shown as 5 min binned intervals. The repeated measures analysis of variance (RMANOVA) are provided for baseline [time: $F(5, 145) = 12.731$, $p < 0.001$; treatment: $F(3, 29) = 2.722$, $p = 0.063$; time by treatment: $F(15, 145) = 1.878$, $p = 0.099$] and for PCP-stimulated activity [time: $F(17, 493) = 22.056$, $P < 0.001$; treatment: $F(3, 29) = 16.992$, $p < 0.001$; time by treatment: $F(51, 493) = 6.159$, $p = < 0.001$]. (B) Locomotor activities presented as cumulative activity (0–30 min) and PCP-stimulated activity (31–90 min). A RMANOVA found the following: [pre–post: $F(1, 29) = 55.625$, $p < 0.001$; treatment: $F(3, 29) = 20.004$, $p < 0.001$; pre–post by treatment: $F(3, 29) = 17.651$, $p < 0.001$]. $N = 8–9$ mice/group; Bonferroni-corrected pair-wise comparisons—*$p < 0.05$, vs baseline within treatment; +$p < 0.05$, vs the Veh-PCP group within the post-stimulation interval; #$p < 0.05$, 1 mg/kg compound vs 3.5 mg/kg compound **38** within the post-stimulation interval.

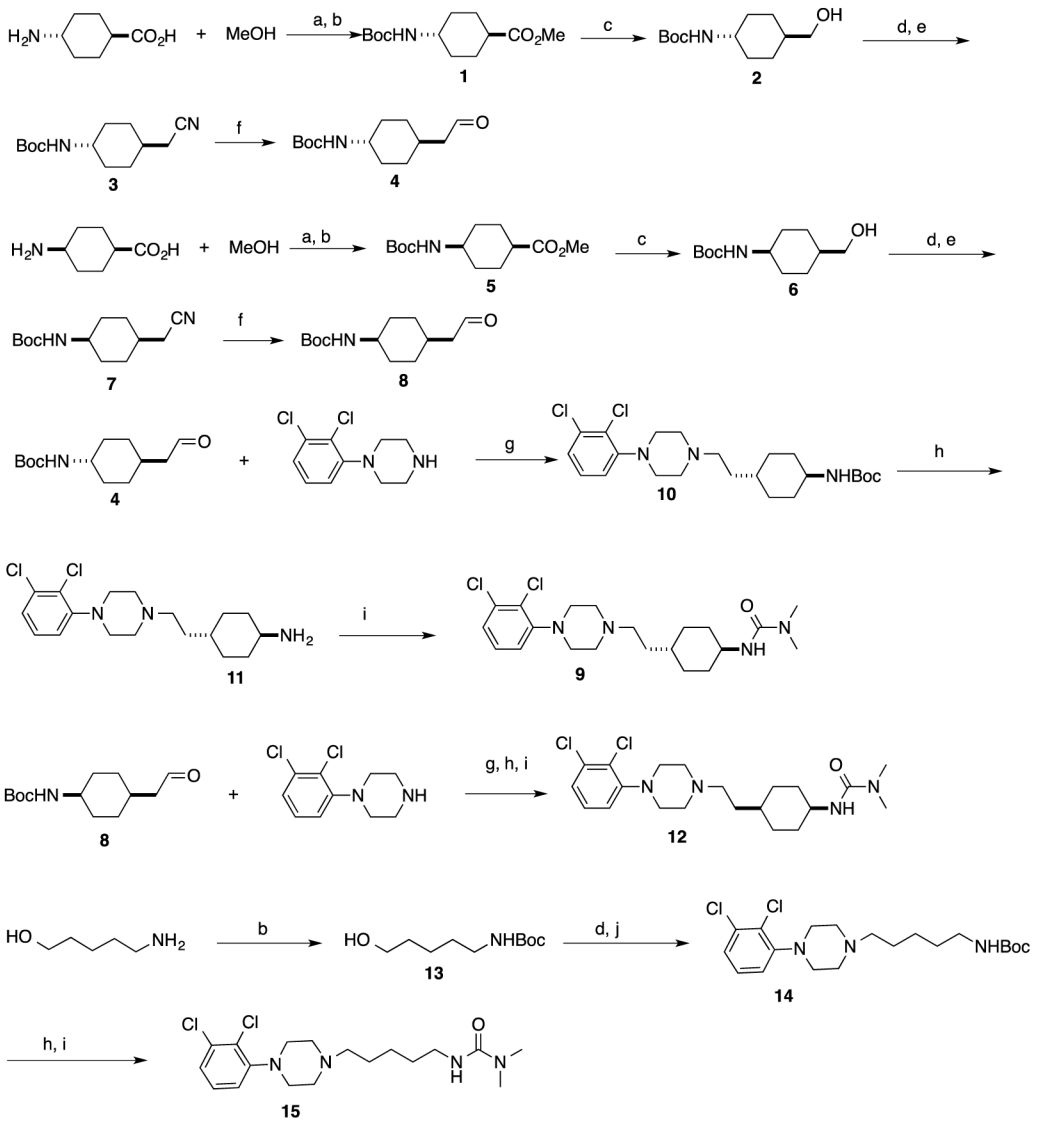

Scheme 1. Synthesis of Cariprazine Analogues[a]

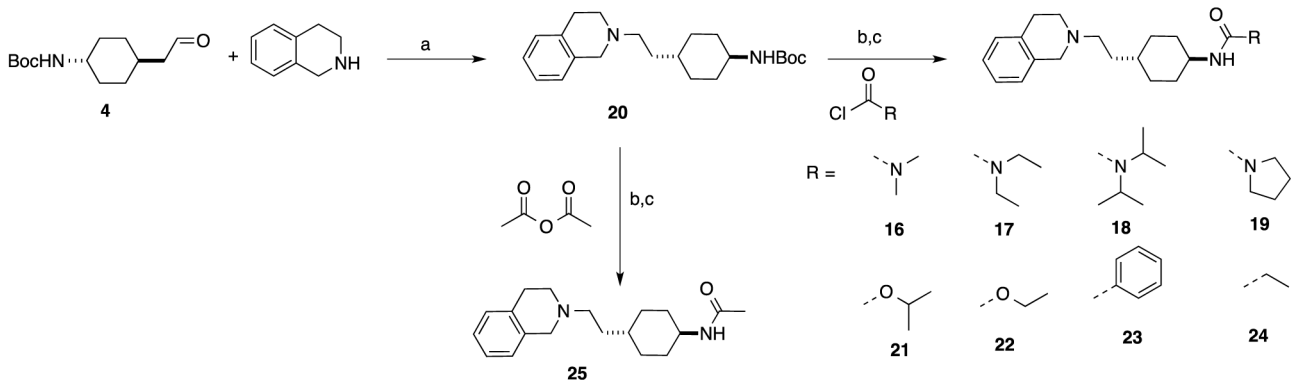

Scheme 2. Synthesis of Compound 6 and Its Analogues 16–25[a]

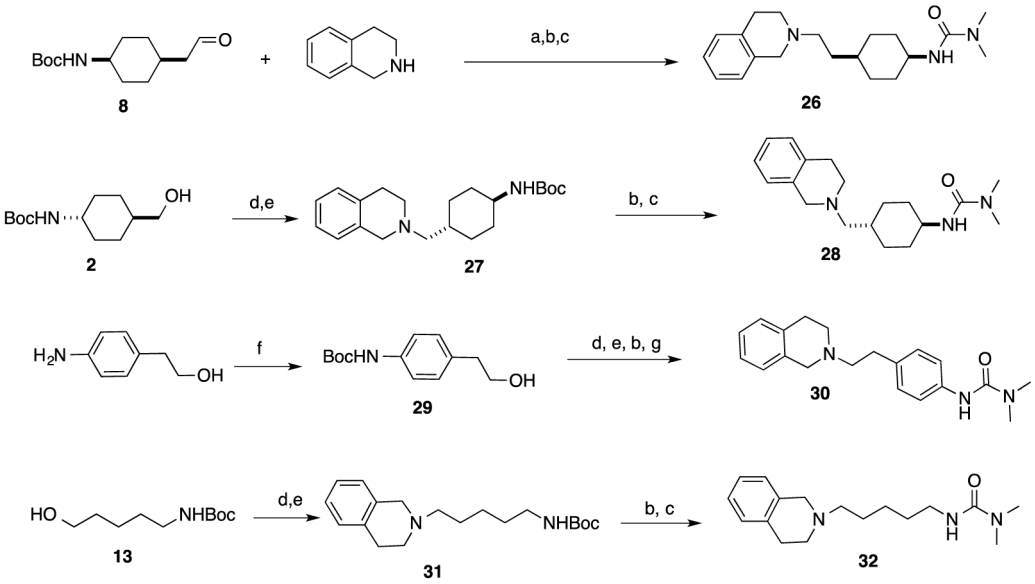

Scheme 3. Synthesis of Compounds for Exploring the Middle Linker[a]

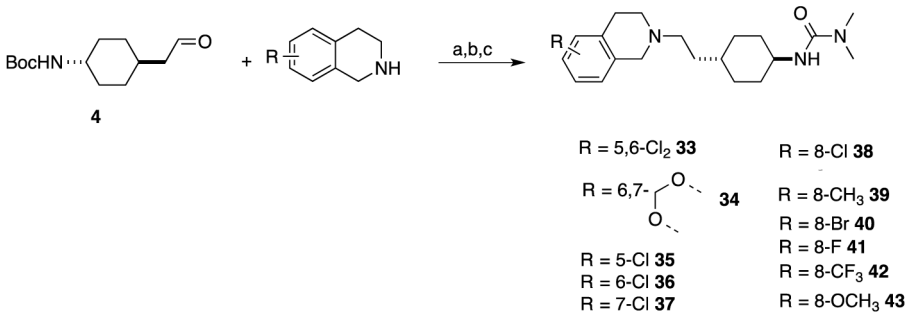

Scheme 4. Synthesis of Compounds with Various Substituents on the LHS Phenyl Ring[a]

Table 1.

SFSR Study on Cariprazine[a]

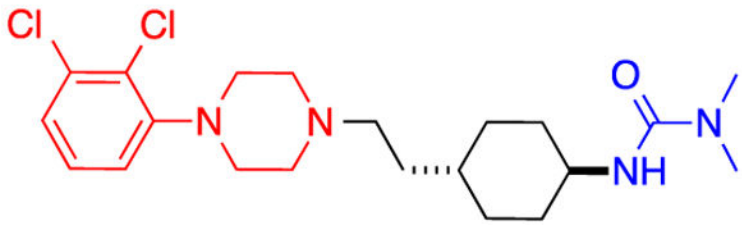

cariprazine (compound **9**)

CPD	Structure	cAMP Inhibition			β-arrestin			Bias for $G_{i/o}$
		EC_{50} (nM)	pEC_{50}	E_{max} (%)	EC_{50} (nM)	pEC_{50}	E_{max} (%)	
9	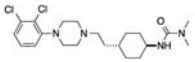	0.4	9.35 ± 0.07	70 ± 1	0.6	9.20 ± 0.09	66 ± 2	1
10	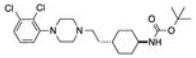	14	7.84 ± 0.07	77 ± 2	9	8.04 ± 0.08	75 ± 2	0.4
11	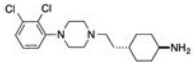	0.7	9.19 ± 0.12	62 ± 2	2	8.71 ± 0.14	64 ± 3	2
12	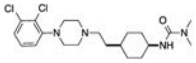	3	8.49 ± 0.11	48 ± 2	12	7.93 ± 0.08	37 ± 1	3
15	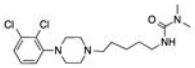	7	8.17 ± 0.24	29 ± 3	10	7.98 ± 0.11	24 ± 1	1
16	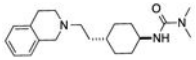	12	7.92 ± 0.11	60 ± 3	69	7.16 ± 0.10	22 ± 1	11

[a] EC_{50}, pEC_{50}, and E_{max} values are the average of at least three independent experiments performed in triplicate with standard error of the mean (SEM). Bias factors were calculated as described in the methods, with respect to quinpirole as a positive control ($G_{i/o}$: EC_{50} = 1.8 nM, pEC_{50} = 8.74 ± 0.08; β-arrestin2: EC_{50} = 2.7 nM, pEC_{50} = 8.57 ± 0.10).

Table 2.

SFSR Study on the Right-Hand Side Moiety of Compound 16[a]

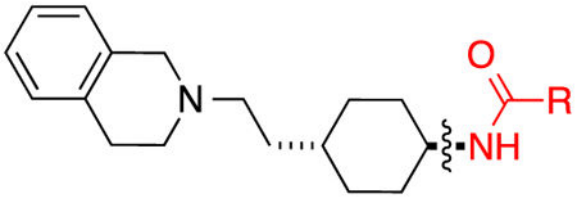

CPD	RHS moiety	cAMP Inhibition			β-arrestin			Bias for $G_{i/o}$
		EC_{50} (nM)	pEC_{50}	E_{max} (%)	EC_{50} (nM)	pEC_{50}	E_{max} (%)	
17	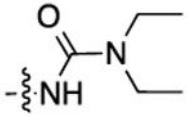	47	7.33 ± 0.27	36 ± 4	312	6.51 ± 0.14	16 ± 1	10
18	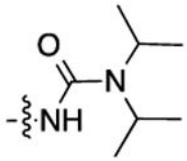	71	7.15 ± 0.17	52 ± 4	183	6.74 ± 0.11	14 ± 1	6
19	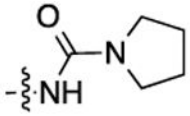	14	7.84 ± 0.14	66 ± 3	88	7.05 ± 0.08	42 ± 1	6
20	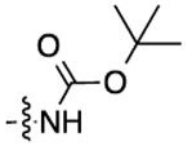	33	7.48 ± 0.08	59 ± 2	195	6.71 ± 0.08	52 ± 3	4

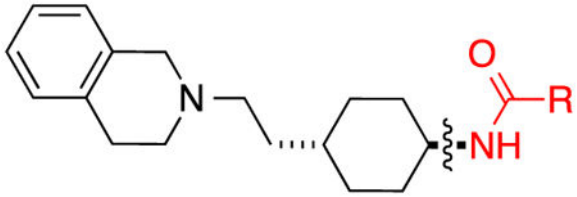

CPD	RHS moiety	cAMP Inhibition			*β*-arrestin			Bias for $G_{i/o}$
		EC_{50} (nM)	pEC_{50}	E_{max} (%)	EC_{50} (nM)	pEC_{50}	E_{max} (%)	
21	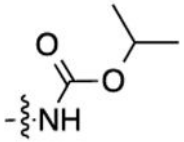	74	7.13 ± 0.21	49 ± 5	238	6.62 ± 0.04	26 ± 1	4
22	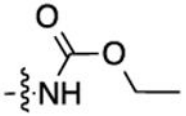	144	6.84 ± 0.15	53 ± 4	636	6.20 ± 0.11	22 ± 1	7
23	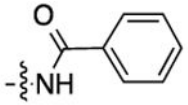	8	8.12 ± 0.13	62 ± 3	65	7.19 ± 0.07	50 ± 2	7
24	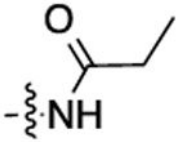	132	6.88 ± 0.28	33 ± 6	N.C.	N.C.	<10	N.C.

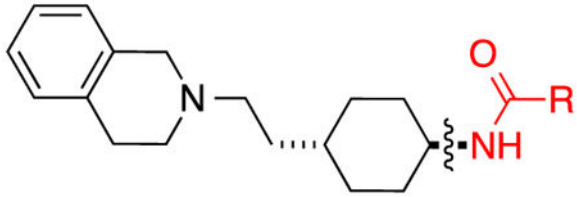

CPD	RHS moiety	cAMP Inhibition			β-arrestin			Bias for $G_{i/o}$
		EC_{50} (nM)	pEC_{50}	E_{max} (%)	EC_{50} (nM)	pEC_{50}	E_{max} (%)	
25	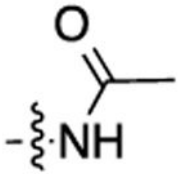	54	7.26 ± 0.36	22 ± 4	N.C.	N.C.	<10	N.C.

[a] EC_{50}, pEC_{50}, and E_{max} values are the average of at least three independent experiments performed in triplicate with standard error of the mean (SEM). Bias factors were calculated as described in the methods, with respect to quinpirole as a positive control ($G_{i/o}$: EC_{50} = 1.8 nM, pEC_{50} = 8.74 ± 0.08; β-arrestin2: EC_{50} = 2.7 nM, pEC_{50} = 8.57 ± 0.10). N.C., not calculated.

Table 3.

SFSR Study of the Middle Linker of Compound 16[a]

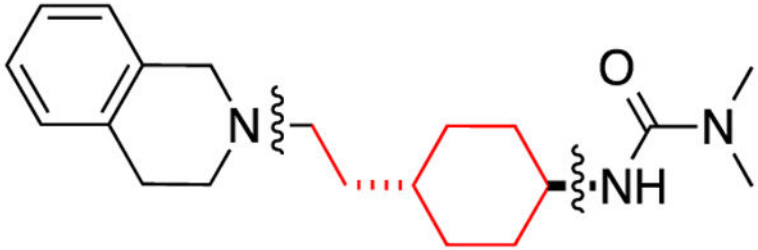

CPD	Middle linker	cAMP Inhibition			β-arrestin			Bias for $G_{i/o}$
		EC_{50} (nM)	pEC_{50}	E_{max} (%)	EC_{50} (nM)	pEC_{50}	E_{max}(%)	
26	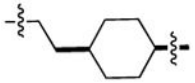	259	6.59 ± 0.15	58 ± 5	>1000	<6.00	N.C.	N.C.
28		N.A	N.A	N.A	N.A	N.A	N.A	N.C.
30	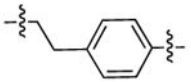	N.A	N.A	N.A	N.A	N.A	N.A	N.C.
32		N.A	N.A	N.A	N.A	N.A	N.A	N.C.

[a] EC_{50}, pEC_{50}, and E_{max} values are the average of at least three independent experiments performed in triplicate with standard error of the mean (SEM). Bias factors were calculated as described in the methods, with respect to quinpirole as a positive control ($G_{i/o}$: EC_{50} = 1.8 nM, pEC_{50} = 8.74 ± 0.08; β-arrestin2: EC_{50} = 2.7 nM, pEC_{50} = 8.57 ± 0.10). N.C., not calculated. N.A., no activity.

Table 4.

SFSR Study of Left-Hand Side Moiety of Compound 16[a]

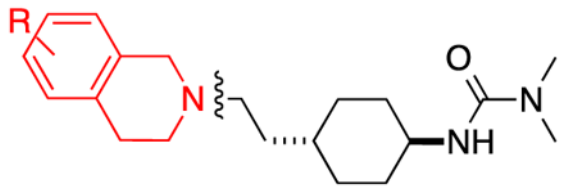

CPD	LHS moiety	cAMP Inhibition			P-arrestin			Bias for $G_{i/o}$
		EC_{50} (nM)	pEC_{50}	E_{max} (%)	EC_{50} (nM)	pEC_{50}	E_{max} (%)	
33	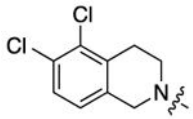	3	8.58 ± 0.05	116 ± 2	2	8.62 ± 0.04	90 ± 1	0.8
34	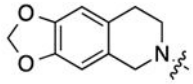	10	8.01 ± 0.08	71 ± 2	26	7.59 ± 0.05	64 ± 1	2
35	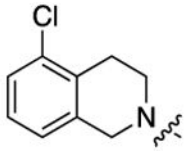	3	8.55 ± 0.05	95 ± 1	4	8.39 ± 0.07	92 ± 2	1
36	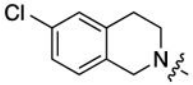	5	8.26 ± 0.16	44 ± 2	17	7.78 ± 0.11	16 ± 1	6
37	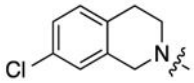	8	8.10 ± 0.16	66 ± 3	5	8.32 ± 0.09	24 ± 1	1

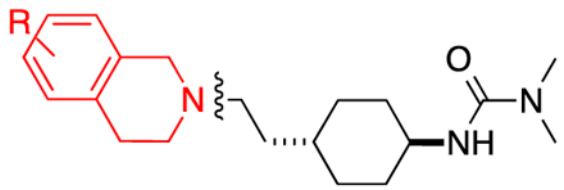

CPD	LHS moiety	cAMP Inhibition			P-arrestin			Bias for $G_{i/o}$
		EC_{50} (nM)	pEC_{50}	E_{max} (%)	EC_{50} (nM)	pEC_{50}	E_{max} (%)	
38	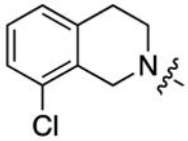	11	7.97 ± 0.13	62 ± 3	40	7.39 ± 0.14	11 ± 1	14
39	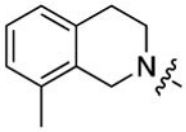	67	7.17 ± 0.09	83 ± 3	N.C.	N.C.	<10	N.C.
40	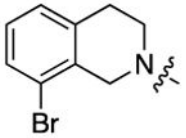	129	6.89 ± 0.09	68 ± 2	N.C.	N.C.	<10	N.C.
41	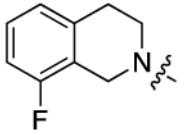	27	7.57 ± 0.00	68 ± 0	60	7.22 ± 0.00	49 ± 1	2
42	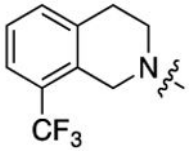	86	7.07 ± 0.16	49 ± 3	202	6.69 ± 0.08	16 ± 1	5

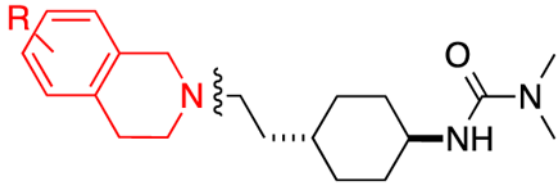

CPD	LHS moiety	cAMP Inhibition			P-arrestin			Bias for $G_{i/o}$
		EC_{50} (nM)	pEC_{50}	E_{max} (%)	EC_{50} (nM)	pEC_{50}	E_{max} (%)	
43	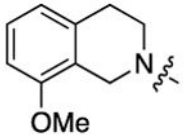	19	7.71 ± 0.07	89 ± 2	54	7.27 ± 0.07	76 ± 2	2

[a] EC_{50}, pEC_{50}, and E_{max} values are the average of at least three independent experiments performed in triplicate with standard error of the mean (SEM). Bias factors were calculated as described in the methods, with respect to quinpirole as a positive control ($G_{i/o}$: EC_{50} = 1.8 nM, pEC_{50} = 8.74 ± 0.08; β-arrestin2: EC_{50} = 2.7 nM, pEC_{50} = 8.57 ± 0.10). N.C., not calculated.